Copyright Warning & Restrictions

The copyright law of the United States (Title 17, United States Code) governs the making of photocopies or other reproductions of copyrighted material.

Under certain conditions specified in the law, libraries and archives are authorized to furnish a photocopy or other reproduction. One of these specified conditions is that the photocopy or reproduction is not to be "used for any purpose other than private study, scholarship, or research." If a, user makes a request for, or later uses, a photocopy or reproduction for purposes in excess of "fair use" that user may be liable for copyright infringement,

This institution reserves the right to refuse to accept a copying order if, in its judgment, fulfillment of the order would involve violation of copyright law.

Please Note: The author retains the copyright while the New Jersey Institute of Technology reserves the right to distribute this thesis or dissertation

Printing note: If you do not wish to print this page, then select "Pages from: first page # to: last page #" on the print dialog screen

A STUDY OF FLUID FLOW ENTERING A SHARP-EDGED CHANNEL

BY

ROCCO RACANO

A THESIS

PRESENTED IN PARTIAL FULFILLMENT OF

THE REQUIREMENTS FOR THE DEGREE

OF

MASTER OF SCIENCE UNDESIGNATED

AT

NEWARK COLLEGE OF ENGINEERING

Newark, New Jersey

1974

ABSTRACT

Experimental investigations were carried out on an almost newtonian fluid in the two dimensional case through the regions of a sharp-edged entrance and exit. Qualitative and quantitative results were compared to a variation of a two dimensional case of converging flow in a capillary as originally derived by Oka and proposed by Philippoff. In addition velocity profiles were taken in the entrance region. Furthermore, the effect of temperature gradients in the slit region with their resulting optical effects were considered. The methods used to obtain these goals were photoelasticity and streak photography.

Results were found to be consistent with the theory for a significantly large range of variation.

APPROVAL OF THESIS

A STUDY OF FLUID FLOW ENTERING A SHARP-EDGED CHANNEL

BY

ROCCO RACANO

FOR

DEPARTMENT OF CHEMICAL ENGINEERING

NEWARK COLLEGE OF ENGINEERING

BY

FACULTY COMMITTEE

APPROVED: _____

_____

_____

NEWARK, NEW JERSEY

JANUARY, 1954

ACKNOWLEDGEMENT

I wish to express deep appreciation and gratitude to Dr. W. Philippoff for his help in the development of the problem and for aid in the evaluation of the results, and to Dr. L. Buteau for his time and assistance in teaching the fundamentals of photoelasticity, his work in the laboratory, and encouragement, all of which was invaluable in the completion of this work.

INDEX

BACKGROUND

While the stress optical law $\Delta n = C \Delta p$ has long been known to be useful for solids, in the past 20 years it has also been extended to liquids. The law states that a material under a stress will produce a value of birefringence proportional to the difference of principal stresses (Δp). The constant of proportionality C is called the stress-optical-coefficient of the material. This stress-optical-coefficient can be measured in the case of simple shearing flow by the equation:

$$\tau_{xy} = \frac{\Delta N}{2C} \sin 2\chi$$

where τ_{xy} = shear stress

ΔN = degree of birefringence

χ = extinction angle

C = stress optical coefficient

τ_{xy} is measured in an instrument consisting of two concentric cylinders of which the inner one is rotating. They are separated by a small gap filled with the liquid to be studied. The motion of the cylinder produces a simple shearing stress in the liquid the magnitude of which is proportional to the velocity at which the cylinder moves. Polarized light is directed through the liquid and through the use of a special optical system consisting of polarizing plates and a half wave plate the amount of birefringence, or the relative retardation, of the traversing rays is

accurately determined. This same procedure by different manipulations will allow for a determination of the extinction angle which occurs when a non-newtonian fluid is under study. For a newtonian liquid the extinction angle is 45 degrees and the sin term in the equation is equal to one. For a viscoelastic fluid the extinction angle will vary with the shear rate and will be different for each fluid.

Indopol H-1900 was used for the following experiments. This liquid is a polybutene (previously called polyisobutylene) and is newtonian except possibly at high shear rates. The concentric cylinder arrangement is far more accurate than any other method in measuring the stress-optical-coefficient and as such was used to determine that of the Indopol.

It was through the work of Lodge[1] and Philippoff[2] that the stress optical laws were developed for liquids. Lodge suggested that the extinction angle and the stress direction were coaxial, Philippoff soon after showed this was indeed true.

Prados and Peebles were interested in finding the velocity profiles in a two dimensional flow system and used

---

[1] A. S. Lodge, "Variation of Flow Birefringence with Stress," Nature, CLXXVI (1955) 838.

[2] W. Philippoff, Nature, 178 (1956), 381.

a birefringent milling yellow dye solution to do so.[3] This common clothing dye is very soluble and the birefringent characteristic made it easy to keep track of. Based on this success the case of accelerated flow of a liquid in a converging channel was investigated by Adams, Whitehead and Bogue utilizing a viscoelastic fluid and photoelastic techniques.[4] Bogue and Peebles soon after did a study of fluid flow using birefringent techniques.[5]

Fields and Bogue have investigated the case of a sharp-edged entrance with a mildly viscoelastic fluid with good agreement to theoretical considerations along the slit centerline.[6] Their upstream reservoir width was too narrow and interfered with their results.

More recent works include those of Drexler and Han,[7]

---

[3]J. W. Prados and F. N. Peebles, "Two Dimensional Laminar-Flow Analysis, Utilizing a Doubly Refracting Liquid," AiChe Journal, V (1959), 225.

[4]E. B. Adams, J. C. Whitehead and D. C. Bogue, "Stresses in a Viscoelastic Fluid in Converging and Diverging Flow," AiChe Journal, XI (1965), 1026.

[5]D. C. Bogue and E. N. Peebles, "Birefringent Techniques in Two Dimensional Flow," Transactions of the Society of Rheology, VI (1962), 317.

[6]T. R. Fields and D. C. Bogue, "Stress Birefringent Patterns of a Viscoelastic Fluid at a Sharp-Edged Entrance," Transactions of the Society of Rheology, XII (1968), 39.

[7]Leonard H. Drexler and Chang Dae Han, "Studies of Converging Flows of Viscoelastic Polymeric Melts Part II. Velocity Measurements in the Entrance Region of a Sharp-Edged Slit Die," Transaction of the Society of Rheology, XVII (1973).

Arai and Asano,[8] and Funatsu and Mori.[9] A summary of all known stress optical laws was given by Philippoff however as they do not directly pertain to the experiments they are not presented here.[10]

As far as is known this work is the first attempted in the field of the flow of an almost newtonian fluid through a sharp-edged entrance and the flow of such investigated in the region of a submerged sharp-edged exit. All predecessors to date have worked with viscoelastic liquids and not nearly newtonian ones.

In addition to this the experiment was principally run to test the theories of Oka who proposed a mathematical solution for the slit entrance problem and the additions and qualifications made by Philippoff for the particular case of a 180° entry.[11] Oka's theories were developed for

---

[8]Teikichi Arai and Hideki Asano, "Analysis of the Flow of Molten Polyethylene Through a Parallel Slit by the Flow Birefringence Method," Chemistry of High Polymers, The Society of Polymer Science, Japan, XXIX, No. 327, (July 1972), 510-514.

[9]Kazumori Funatsu and Yoshiro Mori, "Viscoelastic Stresses in the Flow of Polymer Melt," Chemistry of High Polymers, The Society of Polymer Science, Japan, XXV, No. 278, (1968).

[10]W. Philippoff, "The Present Stand of Rheo-optics of Polymer Solutions," Proceedings of the Fifth International Congress of Rheology, IV (1970).

[11]Syoten Oka, "The Steady Slow Motion of a Viscous Fluid Through a Tapered Tube," Journal of the Physical Society of Japan, XIX (August 1964), 1481-1484.

a newtonian fluid in converging flow, that flow being laminar and the velocity of which being small enough to neglect the inertia terms of the energy equation.

Oka's results, however, applied to a three dimensional capillary and had to be adopted to the case at hand namely two dimensional flow through a slit. The variations or changes were proposed by Philippoff. A short summary of the results for a 180° entry follows.

$$r/r_c = \sqrt{\frac{\cos\theta}{N}}$$

$$\alpha = 3/2\,\theta$$

$$V/V_c = \cos^{3/2}\theta$$

where

r = radius of a run

r_c = reference radius

θ = angle measured from vertical

N = fringe number

α = angle of isocline to vertical

V = velocity of liquid

V_c = reference velocity

Although the equations were developed for a capillary it was felt the results would be reasonably applicable for a slit.

The stress optical laws are developed through the photoelastic technique and the stress optical laws of particular

FIGURE 1

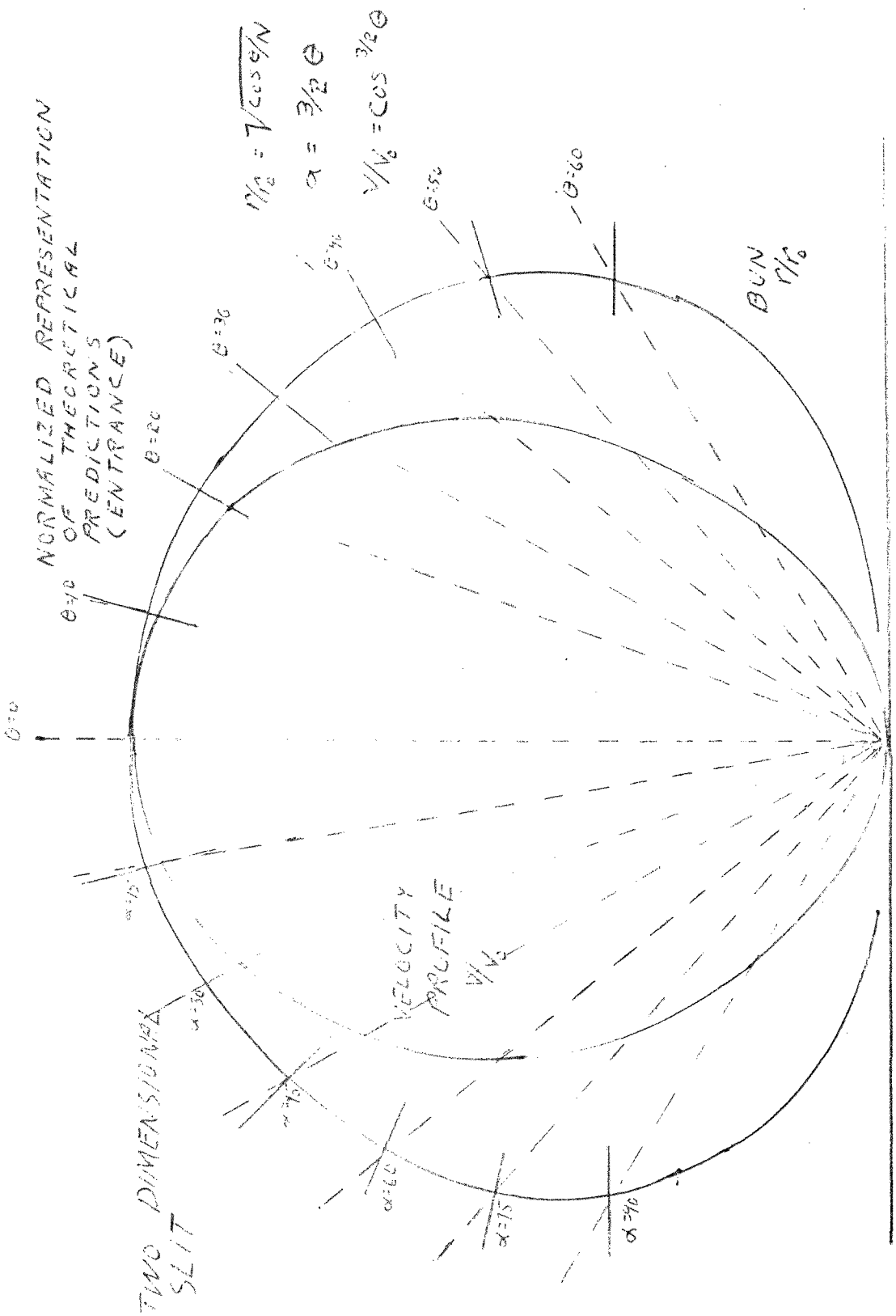
NORMALIZED REPRESENTATION OF THEORETICAL PREDICTIONS (ENTRANCE)
$r/r_2 = \sqrt{\cos\theta/N}$
$\alpha = 3/2\,\theta$
$v/v_0 = \cos^{3/2}\theta$
θ=0
θ=10
θ=30
θ=50
θ=60
θ=76
BUN r/r₀
TWO DIMENSIONAL SLIT
VELOCITY PROFILE v/v₀
α=15
α=30
α=45
α=60
α=75
α=90
SLIT

interest are the shear stress τ_{xy} and the difference in principal stresses $\sigma_1 - \sigma_2$.

The equations for $\sigma_{xx} - \sigma_{yy}$ and τ_{xy} are given from the stress optical law and its transformation to rectangular coordinates as: (see also Han)[12]

$$\tau_{xy} = FN \sin 2\alpha = \frac{\Delta N}{2C} \sin 2\alpha$$

$$\sigma_{xx} - \sigma_{yy} = FN \cos 2\alpha = \frac{\Delta N}{C} \cos 2\alpha$$

where

$F = \lambda / 2C\delta$

N = fringe number

α = angle between principal and normal stresses

λ = wave length

C = stress-optical-coefficient

δ = relative retardation

It was through these equations that Fields and Bogue did their point by point evaluation of the stresses.[13] However, the photoelastic technique gives the directions of σ_1 and σ_2 not σ_{xx} and σ_{yy}.

---

[12] Ibid.

[13] Ibid.

Figure 2

RELATIONSHIP OF PRINCIPAL STRESSES

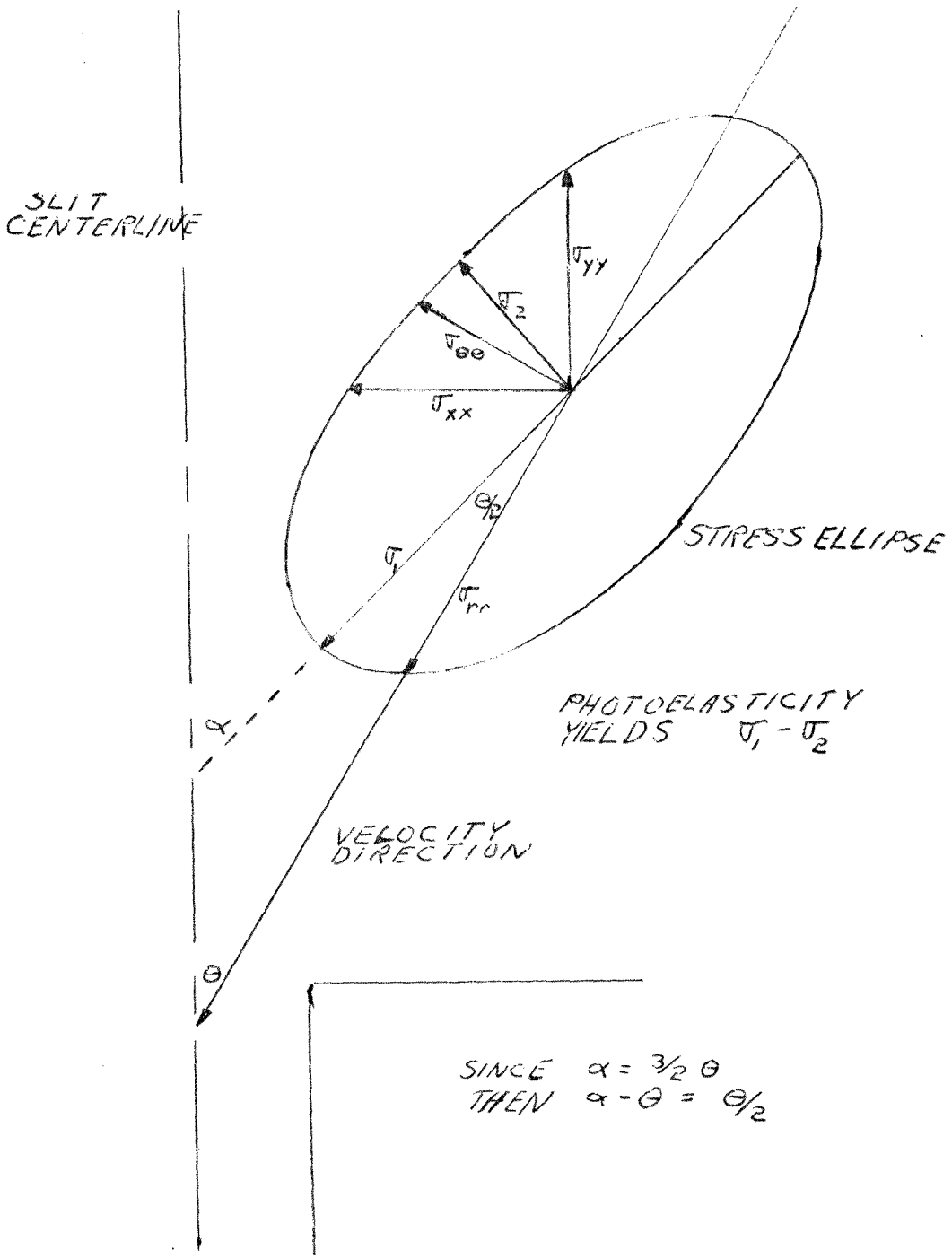

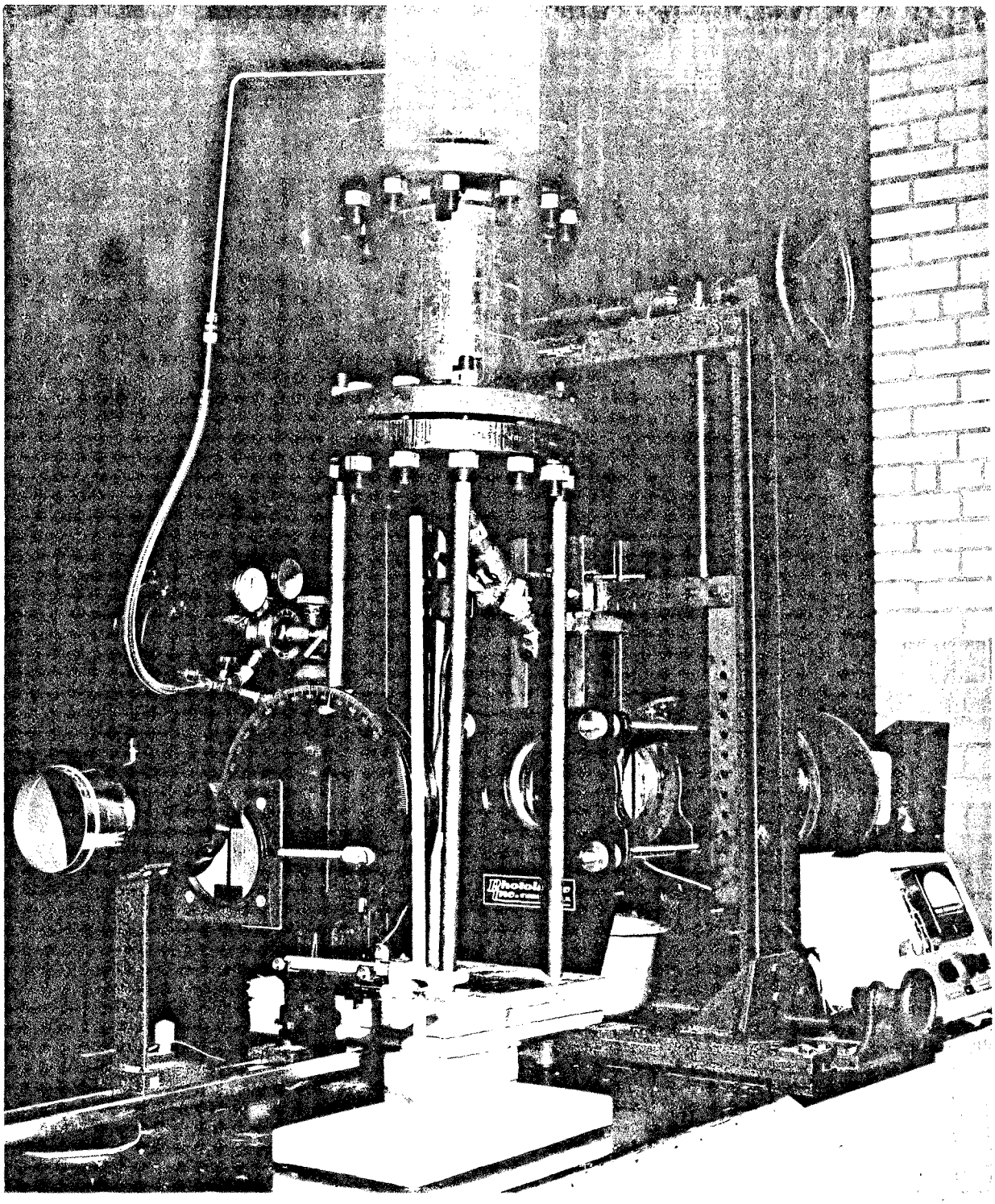

APPARATUS

Test Chamber

The cell was made of stainless steel on all wetted surfaces and carbon steel elsewhere. The slit was 2 3/8" long and nominally 1/8" wide. The length of the slit was determined so as to eliminate any entrance effects at the outlet, the slit width was an average value of all predecessors. The reservoir was 1 ½" wide so as to meet the critical 12:1 ratio of upstream width to slit width that was found by Han and Kim.[14] The ratio is necessary to eliminate flow interference by the side walls. The entry was a 90° sharp corner. The height of the upstream reservoir was 2 7/8" to eliminate possible entrance flow effects in the study area. Provision was made upstream for a baffle but this was found unnecessary. The depth of the cell was 1 ½" to minimize affects of the fluid in contact with the viewing glass. The fluid inlet was a 3/8" diameter opening placed centrally in a trapezoidal volume atop the reservoir. The viewing glass was of 3/4" Vycor which is highly stress resistant. The length of the glass was such that it overextended the exit which allowed for undisturbed viewing of the exit flow. The glass was held in place by contoured carbon steel bolted brackets. The birefringence of the Vycor is small and

---

[14] Ibid.

FIGURE 4

TEST
CELL

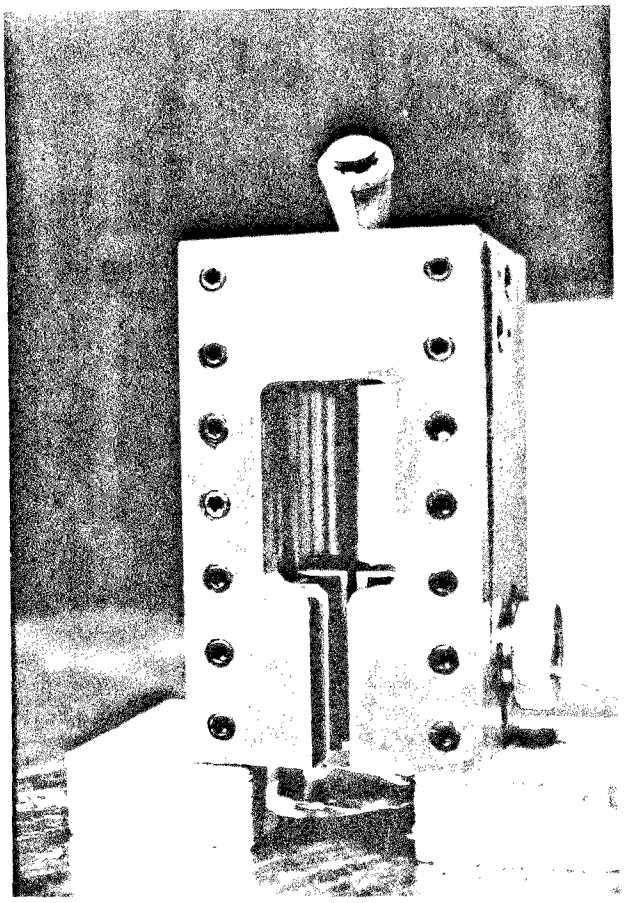

FIGURE 5

TEST
CELL

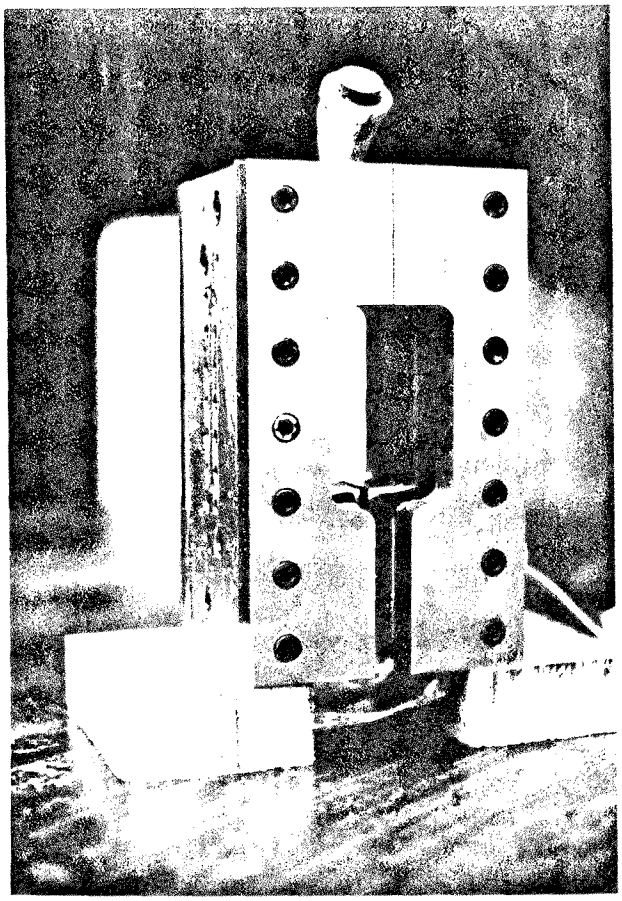

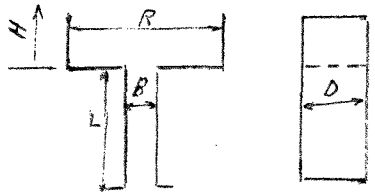

	SLIT DIMENSIONS (CM)					RESERVOIR DIM.		
	B	D	D/B	L	L/B	R	H	R/B
MORI, FUNATSU	0.5	4.0	8	12.5	25	50	8	10
ARAI, ASANO	0.2	2.5	12.5	6.0	30	0.8	6	4
BOGUE, FIELDS	0.42	8.9	21.3	10.2	24.2	1.13	8.9	2.7
HAN CELL *1	0.2	2.0	10.6	1.58	8	2.54	2.54	12.8
HAN CELL *2	0.254	2.54	10.6	5.08	20	1.27	1.27	5
HIRSCH	0.97	6.35	6.5	—	—	—	—	—
N.C.E.	0.318 1/8"	3.18 1 1/4"	10.2 10.2	6.03 2 3/8"	19.65 19.65	3.81 1 1/2"	7.3 2 7/8"	13.3 13.3

FIGURE 7

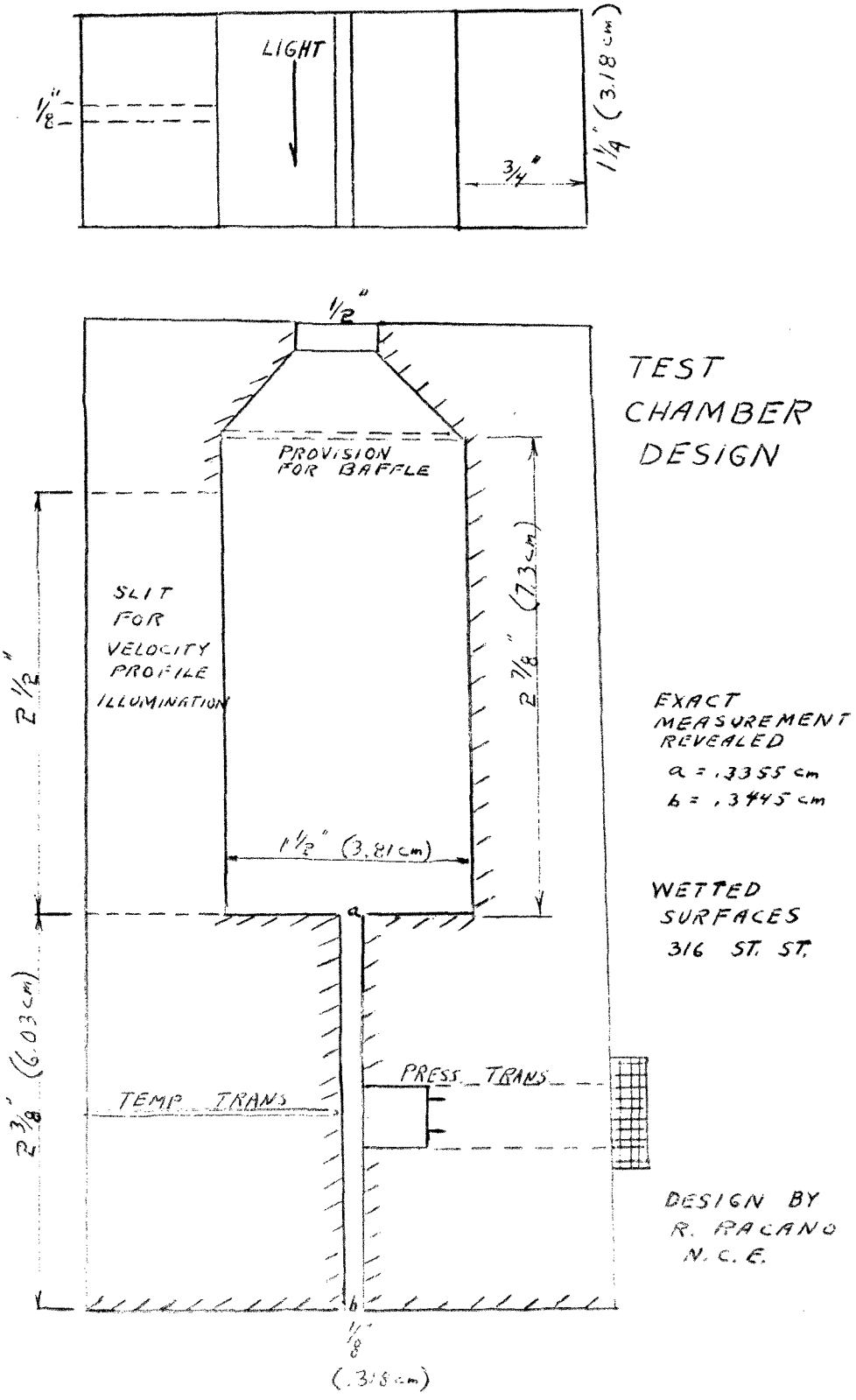
LIGHT
1/8"
3/4"
1/4" (3.18 cm)
1/2"
PROVISION FOR BAFFLE
SLIT FOR VELOCITY PROFILE ILLUMINATION
2 1/2"
2 7/8" (7.3 cm)
1 1/2" (3.81 cm)
2 3/8" (6.03 cm)
TEMP TRANS
PRESS TRANS
1/8"
(.318 cm)
TEST CHAMBER DESIGN
EXACT MEASUREMENT REVEALED
a = .3355 cm
b = .3445 cm
WETTED SURFACES
316 ST. ST.
DESIGN BY
R. RACANO
N. C. E.

found to be negligible.

Provision was made to measure pressure and temperature by electrical means. A pressure transducer was flush mounted at half the length of the slit and a linear thermistor was mounted directly opposite protected by 1/16" of steel. This allowed for a temperature measurement of the slit wall near the fluid.

A slit was made in the upstream reservoir wall at the mid-section of the cell to allow for side lighting of the chamber. This side lighting consideration was introduced to evaluate the velocity profile of the fluid near the slit entrance. The side viewing slit was 1/8" wide and 2 ½" long.

The test cell was designed to withstand an internal static pressure of 1400 psi although this value was not even approached.

A microscopic measurement of the slit width was made to ensure reliability and values of .132" and .136" were made upstream and downstream.

Fluid Supply System

A 1 3/4 gallon (6.6 liters) fluid reservoir was constructed of a 6" diameter nipple and two blank flanges. Pressure was supplied to this reservoir by nitrogen tanks. The pressures reached in the fluid reservoir during the tests never exceeded 400 psi although the system was capable of

much more. The fluid flowed by gravity and pressure to the cell through a 3/4" pipe, a 3/4" ball valve, a 3/4" - 3/8" reducing bushing, and various pipe nipples and elbows. The pressure drop was measured from the fluid reservoir to the slit entrance and found to be 45% of the pressure supplied to the fluid reservoir. The reservoir system was limited to 1000 psi maximum due to the piping.

Optical System

This was a standard polariscope system with small modifications. The light was a 250 watt mercury arc lamp fitted with a green filter to supply 5461A°. This source was made variable by imposing point sources of .025", .050", and .075" diameter in front of the filter at the focus of the collimator. This new point source was placed at the focus of a lens which emitted parallel light. This light was directed through a polarizer and quarter wave plate, the test cell, through a second quarter wave plate and analyser, into a converging lens and finally into a camera with a polaroid back. The variable light source was necessary due to the use of a fringe multiplier (see section on photoelasticity) placed on either side of the test cell which cut down considerably the amount of light transmitted when the unit was placed in the system.

Experiments showed that the time delay element in taking the pictures was very important. As will be seen later a

SCHEMATICAL REPRESENTATION OF TEST SET-UP

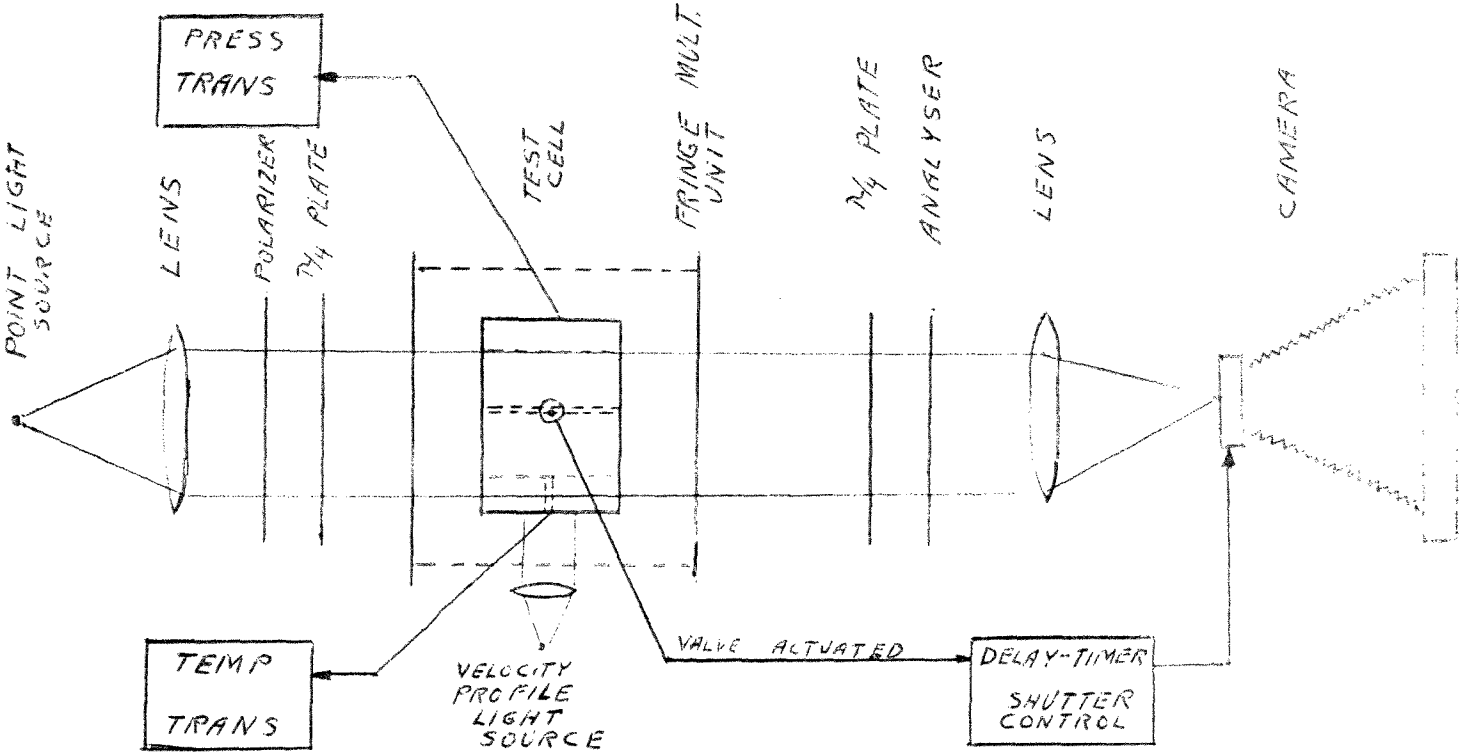

phenomena which shall be called convergence occurred which forced us to have strict control on the time between system operation and the point of shutter release. To solve this problem a switch was placed on the ball valve which activated a variable delay timer of 0 - 1 sec which then tripped the shutter. Trial and error determined the proper delay time to have a fully developed pattern and yet have a minimum of convergence. This was done for each flow rate and condition investigated.

The test cell and fluid reservoir system were mounted to be adjustable in height and alignment and to allow investigation of the exit.

Fluid leaving the exit was collected in a basin and recycled.

Measurements of stress distributions with the use of birefringent techniques have been adopted from solids to liquids by confirmation of the stress optical laws validity in liquids. A short explanation of the workings of the technique follows for those who are unfamiliar with its intricacies.

The particular instrument used in the experiments was a polariscope utilizing monochromatic light and as such the explanation which follows will deal with that particular case.

A monochromatic light point source was placed at the focus of a lens which then emanated parallel light at the test cell. This light is passed through a polarizing plate before the cell which blocks out all light whose electric vectors are not parallel to the plane of polarization. This light then enters the transparent fluid of the cell which is flowing under stress. The fluid Indopol H-1900 is birefringent, i.e., it has the particular property of breaking polarized light into two components, an ordinary and an extraordinary ray which experience a relative retardation that is proportional to the stress at that point.

These waves also have the properties that they are mutually perpendicular and in the directions of principal

stress. This light is now combined by placing an analysing plate at 90^{o} to the polarizer allowing the parallel components of each ray to be transmitted in the same plane. When these light beams are stopped by a camera film, fringe patterns result due to the retardation of the rays. The patterns that result are points where the difference of principal stresses are constant called isochromatics or points where the principal stresses have a common direction called isoclinics.

The light intensity for the above is given by:

$$I = a \sin^2 2 (B - \gamma) \sin^2 \phi/2$$

where

a = magnitude of vector

γ = polarizer angle to reference

B = angle of principal stress

ϕ = phase shift $= \frac{\sigma}{\lambda}(2\pi)$

σ = relative retardation

λ = wavelength

Moving the polarizer and analyzer together will give the isoclinics for that angle of polarization, and the isoclinics that are perpendicular to that orientation angle.

It is desirable, however, that the isoclinics not be visible for certain applications so two quarter wave plates are added to the system one on either side of the test cell inside the polarizer and analyser. These plates are placed

at 90° to each other the first of which is parallel to the polarizer. The resultant equation for the light intensity is given by:

$$I = a^2 \sin^2 \phi/2$$

where the terms are as defined before. Note that the intensity is independent of the direction of the principal stress difference and independent of the extinction angle. This will hold true as long as the quarter wave plates are at right angles to each other. The result is called circular polarized light.

A fairly new technique is that of fringe multiplication where by the use of partially reflecting mirrors set at a slight angle to each other you can capture on film an image that is formed after a wave of light has passed through the cell an odd number of times and hence experienced 1, 3, 5, 7, ... times the amount of birefringence it would normally. This allows fractional fringe numbers to be read directly. This technique coupled with the utilization of light and dark field pictures with the circular polariscope, and pictures with linearly polarized light comprised the experimental techniques used.

A recent addition to the technique consists of using a laser to produce a holograph showing interference patterns

of $\sigma_1 + \sigma_2$.[15]

As a result of all of the above the photoelastic technique is a powerful tool for evaluation of stress distributions at almost any point in a flow field.

---

[15]R. J. Sanford and A. J. Durelli, "Interpretation of Fringes in Stress-Holo-Interferometry," Experimental Mechanics, (April 1971), pp. 161-166.

EXPERIMENTAL

Using the set up as shown in Fig. (8) the fluid was allowed to flow with fluid reservoir pressures of 100, 200, 300, and 400 psi. The optimum delay time was determined for each pressure by trial and error so that the convergence was minimized yet a fully developed pattern was visible. Under these conditions pictures were then taken of the isochromatics at the entrance and exit. In addition isoclinics were found through the use of plane polarized light and taken at orientation angles of 0°, 15°, 30°, and 45°. The results were amplified through the use of light and dark fields giving full and half orders and through the use of the fringe multiplier with light field giving the 1/6, 1/2, 5/6, ... fringe orders.

Intermediate pressures were used to fill in wherever needed in the data and the technique of fringe sharpening (by use of partially reflecting mirrors the light intensity can be manipulated so as to give sharper changes in intensity and hence sharpen the fringe) was tried with little effect.

In the exit pictures a fluid to air exit was initially tried with the result that the fluid separated from the glass and made measurements difficult. To remedy this a submerged exit was created by forming a reservoir at the exit by use of a suspended plate. In this way the fluid

contacted the glass throughout the area in interest.

In regards to the convergence this was investigated thoroughly and found not to be the result of an experimental error but rather an associated phenomena. Tests showed that its effect increased with the rate of shear and was visible only above 138 psi drop on the slit.

The effect was also a superimposed one, i.e., it was independent of the isochromatic pattern. This was discovered when by the use of a high light intensity it was found that the effect could be burned through to show the underlying stress pattern. This technique could not be utilized to eliminate the convergence, however, since the resulting pictures were of such low quality. It was formulated that the convergence was due to a temperature gradient near the walls of the slit which affected the fluids index of refraction. The temperature rise needed was only of the order of $2^{\circ}F$ due to the high change of index of refraction with temperature of the liquid. Methods to measure temperature differences were then developed.

Available for use was the thermistor mounted in the cell and a copper-constantan thermocouple made of 5 mil wire and 5 mils in size which was mounted so to traverse the exit of the cell. Due to the high viscosity (5200 poises) of the Indopol the thermocouple was rendered useless. The Indopol would form a stagnant layer around the

thermocouple and impede the measurements. The thermistor was taken from its mount and brought so that it would just contact the emerging stream of fluid and in this way the temperature was measured. The change was found to be small.

If a change of index of refraction occurred it should break white light into its components scattering red light toward the camera. White light was then used and red light was not observed in the area of convergence. The convergence then remained unexplained. The possibility of temperature stratification in the room is foremost among remaining possibilities.

Velocity profiles were made by shining parallel light through the slit made for that purpose. This allowed velocity measurements of a narrow slice in the center of the cell (this center profile was found to be necessary after a trial of Han's technique of streak photography was found to give only scattered points with no possibility of drawing conclusions[16]). This technique was not new and hopefully eliminated or made negligible the effects of the glass on the velocity profile in the fluid.[17] An exposure of measured

---

[16] Ibid.

[17] David R. Rea, and W. R. Schowalter, "Velocity Profiles of a Non-Newtonian Fluid in Helical Flow," Transactions of the Society of Rheology, XI-1 (1967), 125-143.

time interval was then made with the fluid flowing and the velocity measured by measuring the length of the streak created by the nitrogen bubbles that were dissolved in the system. The positions of the nitrogen bubbles were random and hence many pictures were required to obtain a velocity profile. The nitrogen bubbles formed due to the inherent pressure drop in the system.

Due to the compact size of the Polaroid pictures all measurements were taken with the aid of a microscope equipped for calibrated measurement. It was felt if these pictures were reproduced on a larger scale photographically from the Polaroid pictures that too much loss of detail or possible unaccountable distortion would result. The option of optical magnification was not available due to the lack of necessary equipment.

Figure 9

INDOPOL H-1900 Viscosity Data

Temperature		Viscosity
^{o}F	^{o}C	(poises)
77	25	5048.6
85.7	29	3250.3
86	29.4	3196.5
100	37.8	1663.0
113	45	931.1
130	54.4	459.2
149	65	225.1
167	75	120.5
194	90	52.6

The Stress-Optical-Coefficient

C = 1340 Brewsters (constant for low temperatures)

FLOW RATE Q (cc/min)

RESERVOIR PRESSURE	Q CALCULATED 77°F	Q MEASURED 80°F
100	126.46	122.8
200	252.92	246.2
300	379.38	351.7
400	499.30	465.0

THE SHEAR STRESS IN THE SLIT IS GIVEN BY $\tau = \frac{Pa}{2L} = \frac{69{,}000\,(.3345)(P)(.551)}{2\,(6.03)}$

$$\tau = 1054.5\,(P)$$

THEN $\dot{\gamma} = \tau/\mu$ $\quad \dot{\gamma}$ = RATE OF SHEAR, μ = VISCOSITY

ALSO $\dot{\gamma} = \frac{6Q}{ba^2}$ $\quad b = 3.28$ cm, $a = .3345$ cm

YIELDING

$$\dot{\gamma} = .270857\,Q \quad \text{OR} \quad Q = 3.691972\,\dot{\gamma}$$

$$\bar{V} = \frac{Q}{(.3345)(3.18)} = .940105855\,Q$$

$$V_{MAX} = 2\bar{V} \quad (cc/_{MIN})$$

.551 = FRACTION OF RESERVOIR PRESS. ON THE SLIT

RESERVOIR PRESSURE PSI	SLIT PRESS DROP PSI	SHEAR STRESS τ DYNES/CM^2	RATE OF SHEAR SEC^{-1}	FLOW RATE Q (CC/MIN)	FLOW RATE Q (CC/SEC)	AVERAGE VEL. $\bar{V}$ (CM/SEC)	MAX. VEL. V_{MAX} (CM/SEC)
30	17	32×10^3	9.73	35.9	.59	.56	1.12
50	23	53×10^3	16.22	59.9	1.00	.93	1.86
70	36	74×10^3	22.71	83.8	1.41	1.31	2.62
100	55	111×10^3	34.25	126.5	2.11	1.96	3.92
150	78	165×10^3	50.79	187.5	3.11	2.93	5.86
200	110	223×10^3	68.50	252.9	4.21	3.95	7.90
250	133	278×10^3	85.63	316.2	5.26	4.95	9.90
300	165	334×10^3	102.76	379.4	6.31	5.93	11.86
350	188	387×10^3	119.29	440.4	7.33	6.90	13.80
400	229	440×10^3	135.24	499.3	8.31	7.81	15.62

AVG. SYSTEM PRESSURE LOSS 55.1%

VELOCITY MEASUREMENTS IN THE ENTRANCE REGION OF A SLIT DIE

Due to the small sizes of the fluid reservoir and slit, velocity measurements became a major problem in the experiment. The use of any kind of measuring instruments was ruled out due to the small sizes. The flow was laminar and radial in the region to be investigated from the equation of continuity then the velocity had to vary as the reciprocal of the radius for accelerated flow.

Han in his work introduced foreign particles to the fluid.[18] These particles were small enough in diameter so as to not affect the flow and their specific gravity picked to be close to that of the liquid involved and therefore not move with a different velocity. Han's fluid was viscoelastic versus our newtonian one. Other velocity measurement methods were cited by Han. Of these only one was used for a newtonian fluid, and was developed by Frantisak.[19] This consisted of dissolving a photochromatic dye in the liquid and irradiating it with ultraviolet light. In light of the unfamiliarity we had of this system it was ruled out.

Getting back to Han's work it was noted that he used a polymer melt which differed from us. Also to illuminate

---

[18] Ibid.

[19] M. Frocht, Photoelasticity, vol. 1, John Wiley and Sons, Inc., New York, N. Y. (1941).

the system for his streak photography technique Han used a light source located at 60° to and above the cell. This lighting technique restricted Han to illuminating the entire cell including the liquid in contact with the glass walls. The fluid in contact with or near the glass walls moves with a smaller velocity than the mainstreams of fluid. This also was noted by Han and compensated for by using the average value of the velocity found for each point. Since there is no way to determine the thickness of the slower moving layers a weighted average is impossible and an error results. Having known this beforehand provision was built into our test cell to allow a center slice of the liquid to be lit while keeping the outer planes in darkness.

Unmentioned by Han was the technique of using nitrogen bubbles instead of suspended particles to determine velocity. This alternative was a ready and practically viable solution to our problem. Nitrogen gas was used as our pressure source and as a result of long experiments was continually being dissolved in our system. Our system also had an inherent 45% pressure loss which served to form the nitrogen into small bubbles. These bubbles when lit from the side (a 100 watt light source with a collimating lens was used) would create a spot of light, if the fluid was moving a streak of light. It was not restricted only to the thin slice (.125 inches) in the center however but lit up bubbles outside this range as well. These extremes, however, could easily

be singled out by eye as they were not as intense as the others. In this way the slower moving layers near the glass walls were virtually removed.

Due to the relatively slow exposure times, the shutter speeds posted on the camera could not be taken as accurate. As a check a light source was placed on one side of the shutter and a photocell on the other. The iris was a part of the shutter and was also in this set up at the proper setting. The shutter was then tripped and the output of the photocell was captured on an oscilloscope and the shutter calibrated in this manner.

It is felt our technique was the most accurate of all available. One drawback was the inaccuracy due to the acceleration of the particles which served to lengthen the streaks.

Several attempts were made to eliminate this by double exposing the picture after a known time delay producing pairs of bubbles but this system was found to be difficult due to the large number of bubbles which made matching pairs close to impossible.

INDEX TO PICTURES

1. (a) Fringe multiplication of entrance 2.1cc/sec., $\tau = 1.11 \times 10^5$ dynes/cm^2
   (b) " " " " 4.2cc/sec., $\tau = 2.23 \times 10^5$ dynes/cm^2
   (c) " " " " 6.3cc/sec., $\tau = 3.34 \times 10^5$ dynes/cm^2
   (d) " " " " 8.3cc/sec., $\tau = 4.4 \times 10^5$ dynes/cm^2
2. (a) Light field of entrance 2.1cc/sec., $\tau = 1.11 \times 10^5$ dy/cm^2
   (b) " " " " 4.2cc/sec., $\tau = 2.23 \times 10^5$ dy/cm^2
   (c) " " " " 6.3cc/sec., $\tau = 3.34 \times 10^5$ dy/cm^2
   (d) " " " " 8.3cc/sec., $\tau = 4.4 \times 10^5$ dy/cm^2
3. (a) Dark field of entrance 2.1cc/sec., $\tau = 1.11 \times 10^5$ dy/cm^2
   (b) " " " " 4.2cc/sec., $\tau = 2.23 \times 10^5$ dy/cm^2
   (c) " " " " 6.3cc/sec., $\tau = 3.34 \times 10^5$ dy/cm^2
   (d) " " " " 8.3cc/sec., $\tau = 4.4 \times 10^5$ dy/cm^2
4. (a) 0° Isoclinics at entrance 8.3cc/sec., $\tau = 4.4 \times 10^5$ dy/cm^2
   (b) 15° " " " " "
   (c) 30° " " " " "
   (d) 45° " " " " "
5. (a) Dark field of entrance .59cc/sec., $\tau = .37 \times 10^5$ dy/cm^2
   (b) " " " " 1.0cc/sec., $\tau = .55 \times 10^5$ dy/cm^2
   (c) " " " " 1.4cc/sec., $\tau = .78 \times 10^5$ dy/cm^2
   (d) " " " " 2.1cc/sec., $\tau = 1.11 \times 10^5$ dy/cm^2
6. (a) Light field of exit (air) 2.1cc/sec., $\tau = 1.11 \times 10^5$ dy/cm^2
   (b) " " " " " 4.2cc/sec., $\tau = 2.23 \times 10^5$ dy/cm^2
   (c) " " " " " 6.3cc/sec., $\tau = 3.34 \times 10^5$ dy/cm^2
   (d) " " " " " 8.3cc/sec., $\tau = 4.4 \times 10^5$ dy/cm^2

7. (a) Dark field of exit (air) 2.1cc/sec., $\tau = 1.11 \times 10^5$ d/cm^2
   (b) " " " " " 4.2cc/sec., $\tau = 2.23 \times 10^5$ d/cm^2
   (c) " " " " " 6.3cc/sec., $\tau = 3.34 \times 10^5$ d/cm^2
   (d) " " " " " 8.3cc/sec., $\tau = 4.4 \times 10^5$ d/cm^2
8. (a) 0° Exit (air) isoclines 8.3cc/sec., $\tau = 4.4 \times 10^5$ d/cm^2
   (b) 15° " " " " "
   (c) 30° " " " " "
   (d) 45° " " " " "
9. (a) Light field of exit (submerged) 2.1cc/sec., $\tau = 1.11 \times 10^5$ d/cm^2
   (b) " " " " " 4.2cc/sec., $\tau = 2.23 \times 10^5$ d/cm^2
   (c) " " " " " 6.3cc/sec., $\tau = 3.34 \times 10^5$ d/cm^2
   (d) " " " " " 8.3cc/sec., $\tau = 4.4 \times 10^5$ d/cm^2
10. (a) Dark field of exit (submerged) 2.1cc/sec., $\tau = 1.11 \times 10^5$ d/cm^2
   (b) " " " " " 4.2cc/sec., $\tau = 2.23 \times 10^5$ d/cm^2
   (c) " " " " " 6.3cc/sec., $\tau = 3.34 \times 10^5$ d/cm^2
   (d) " " " " " 8.3cc/sec., $\tau = 4.4 \times 10^5$ d/cm^2
11. (a) 0° Exit (submerged) isoclines 8.3cc/sec. $\tau = 4.4 \times 10^5$ d/cm^2
   (b) 15° " " " " "
   (c) 30° " " " " "
   (d) 45° " " " " "
12. (a) 0° Entrance isoclines 3.1cc/sec., $\tau = 1.67 \times 10^5$ d/cm^2
   (b) 15° " " " "
   (c) 30° " " " "
   (d) 45° " " " "

13.(a) 0° Entrance isoclines 4.2cc/sec. $\Sigma = 2.23 \times 10^{5}\ d/c_4$

(b) $22\frac{1}{2}^{\circ}$ " " " "

(c) 45° " " " "

(d) Entrance no flow condition showing streamlines.

14. Velocity streak photography 4.2cc/sec.

Exposure time .23 seconds.

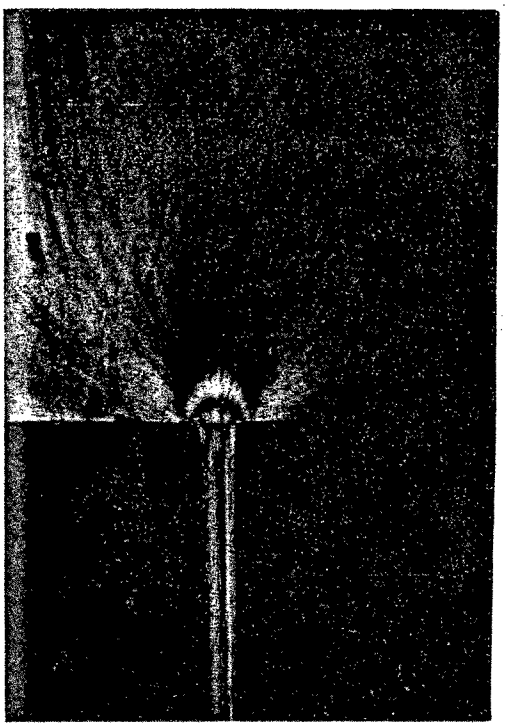

1A

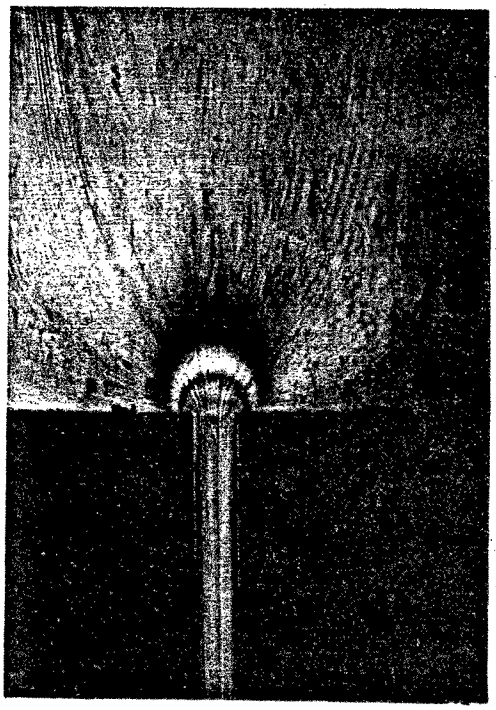

1B

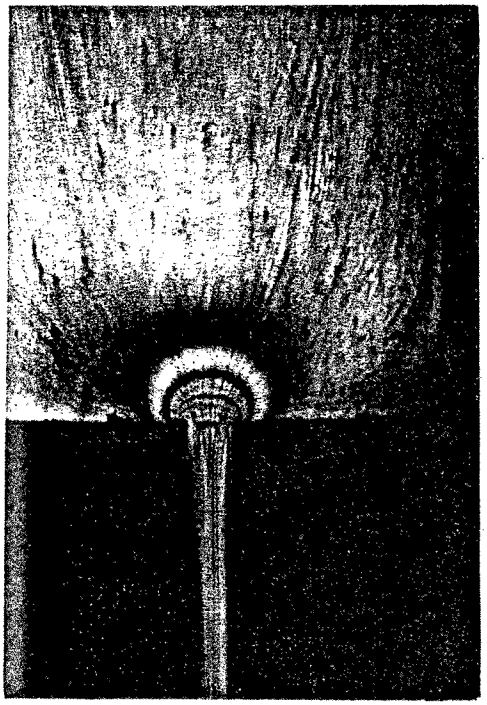

1C

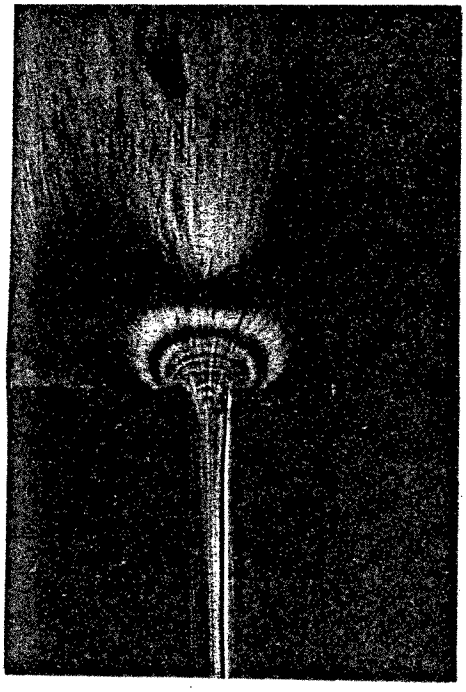

1D

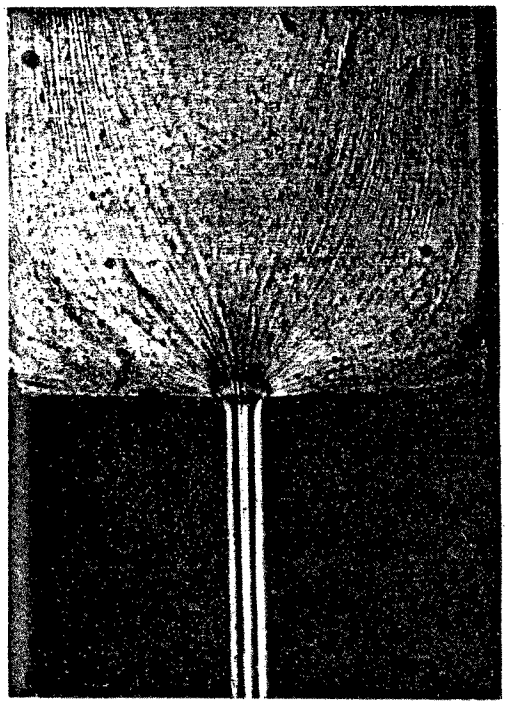

2A

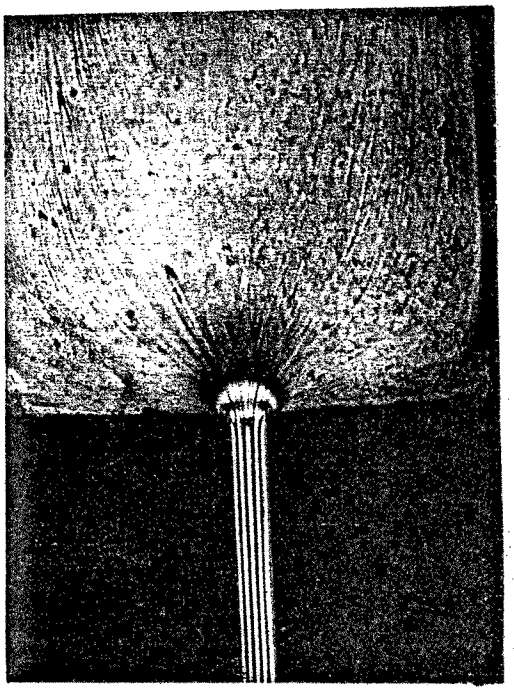

2B

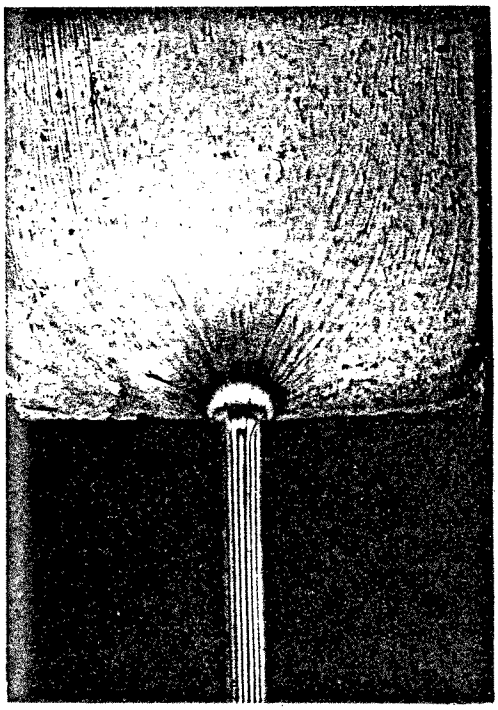

2C

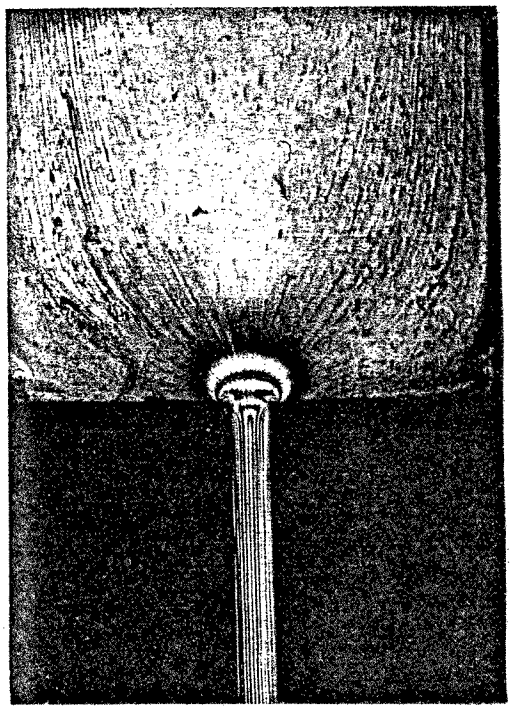

2D

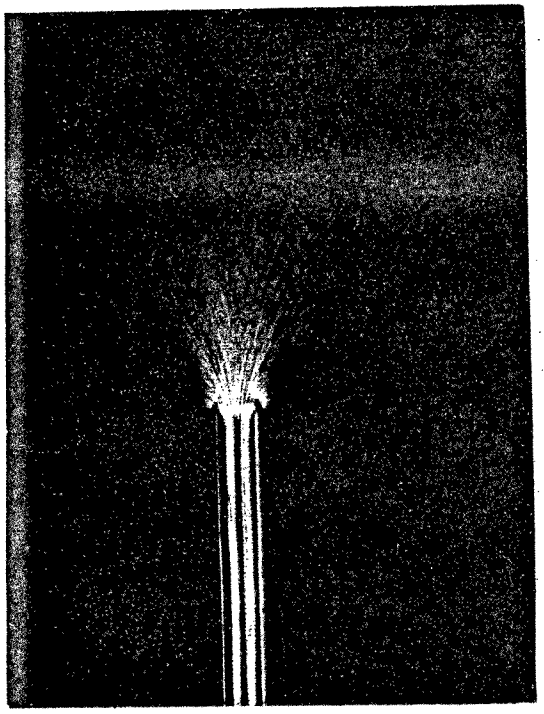

3A

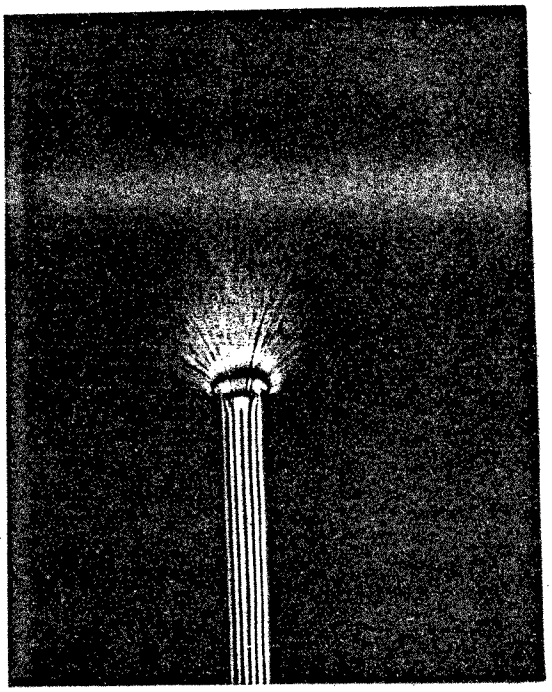

3B

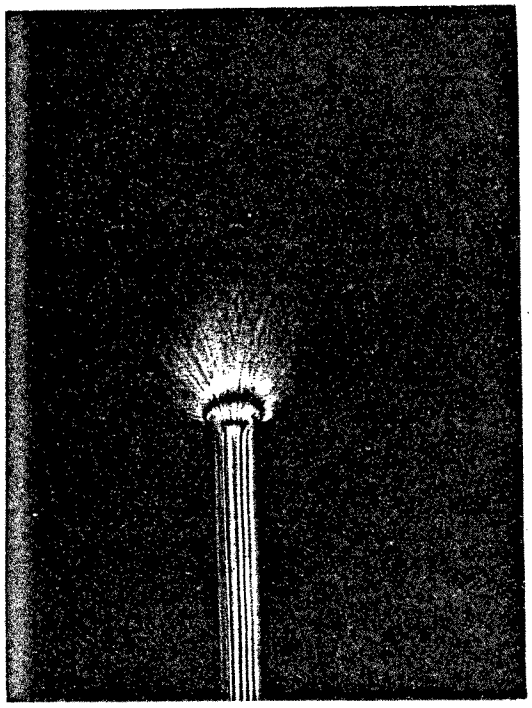

3C

3D

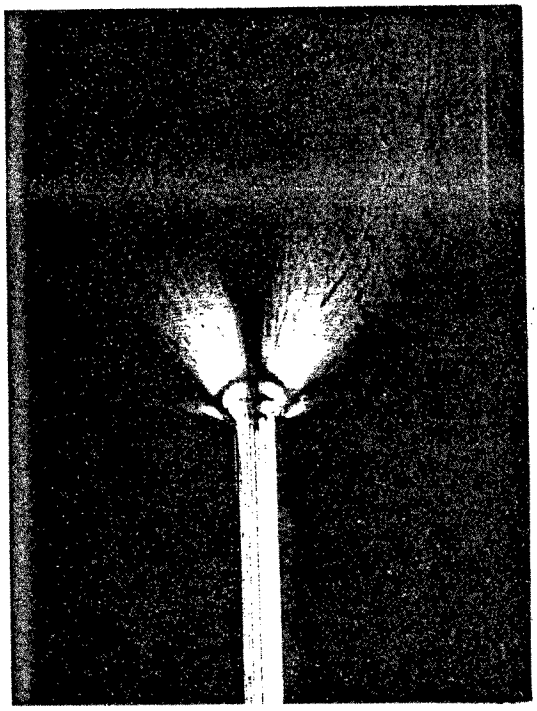

4A

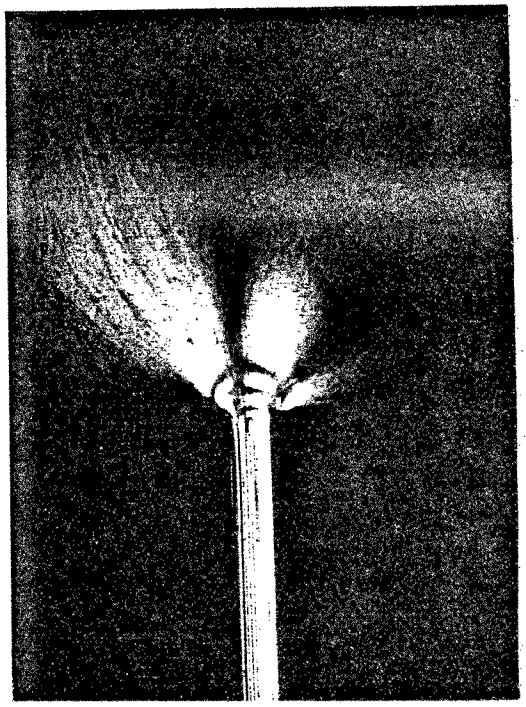

4B

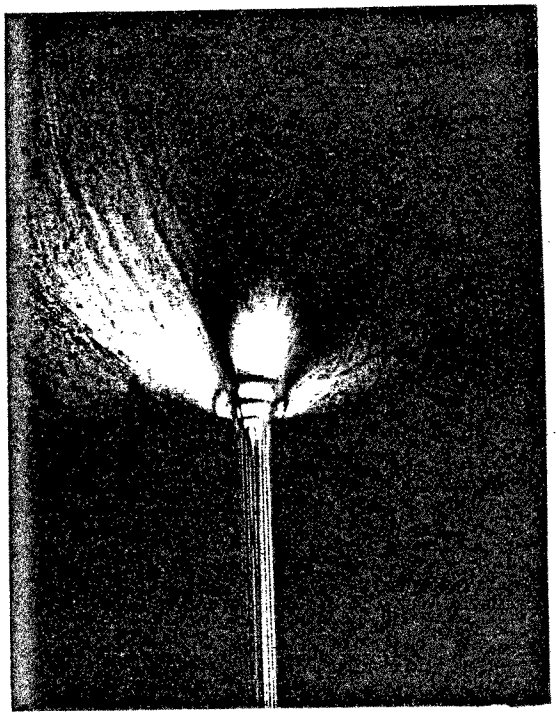

4C

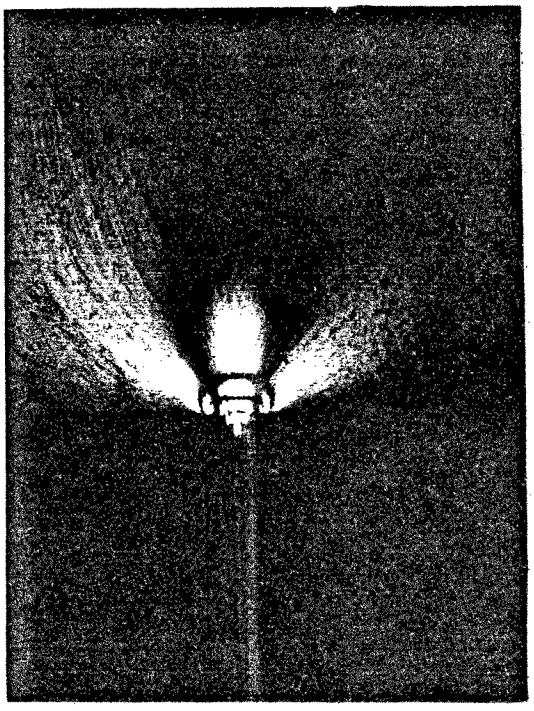

4D

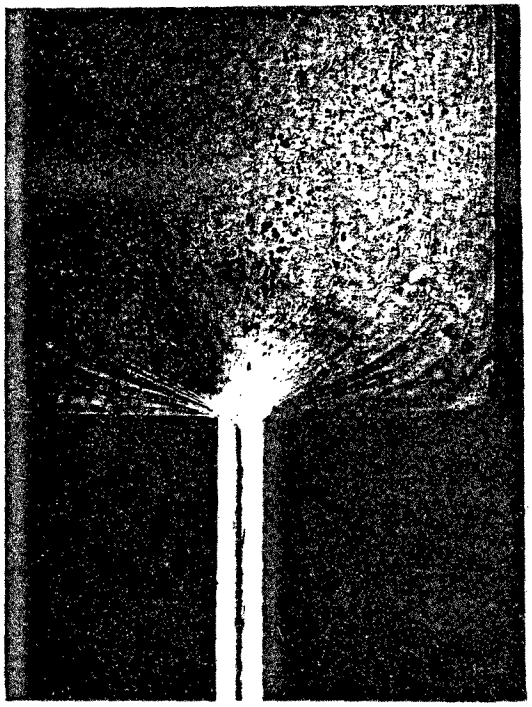

5A

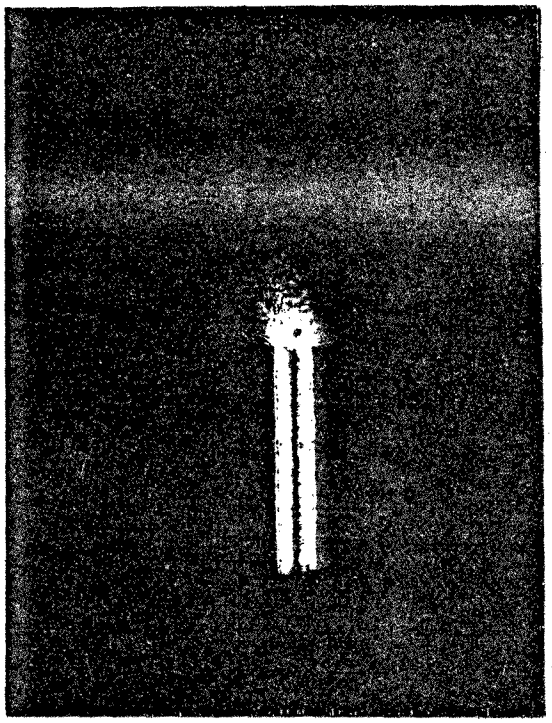

5B

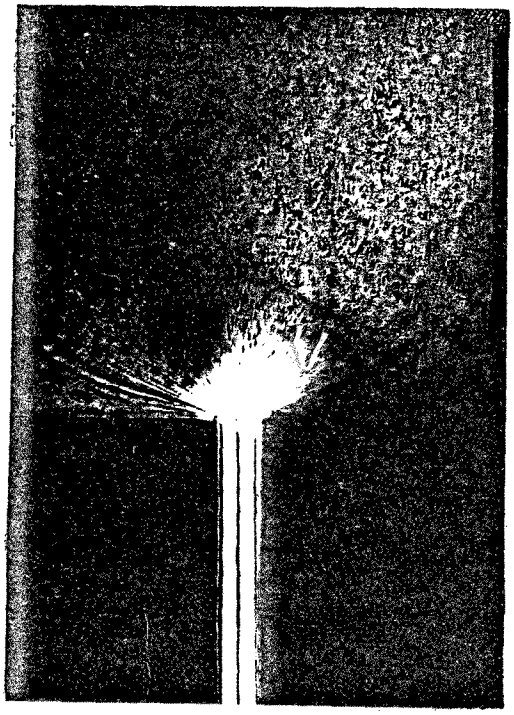

5C

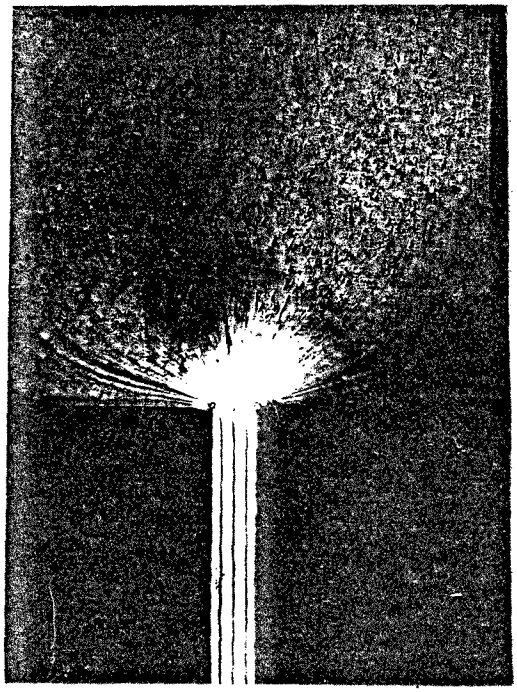

5D

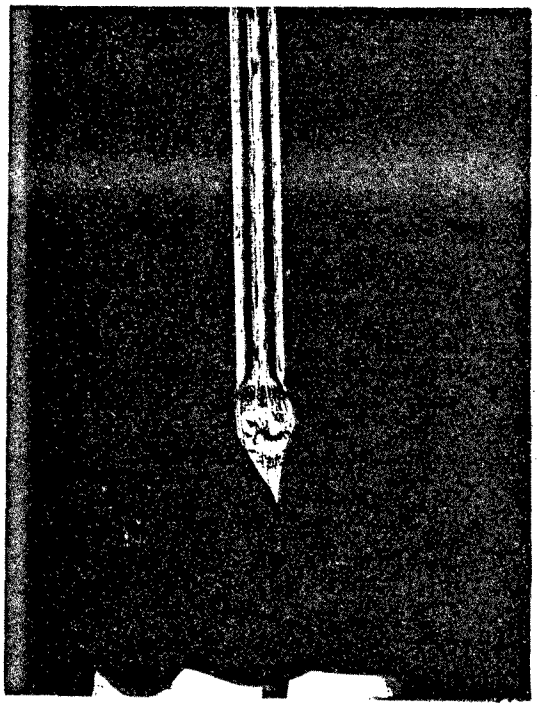

6A

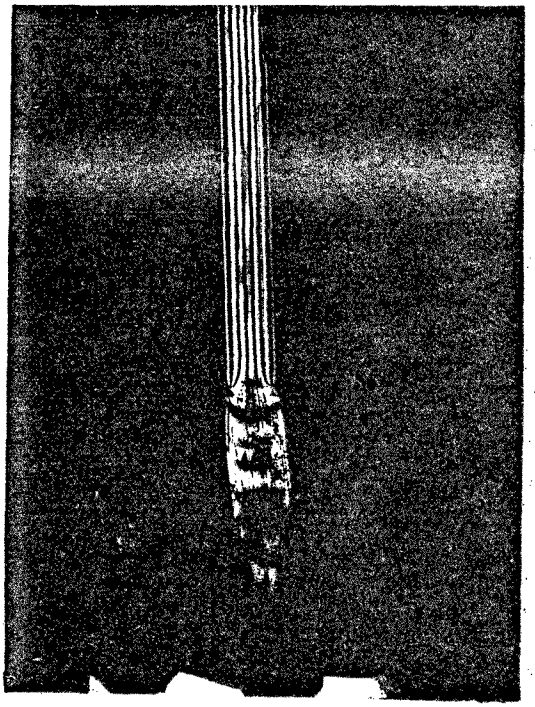

6B

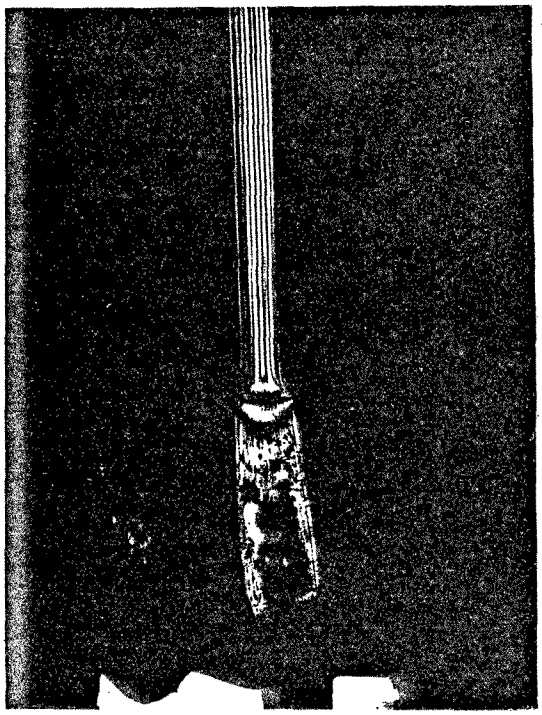

6C

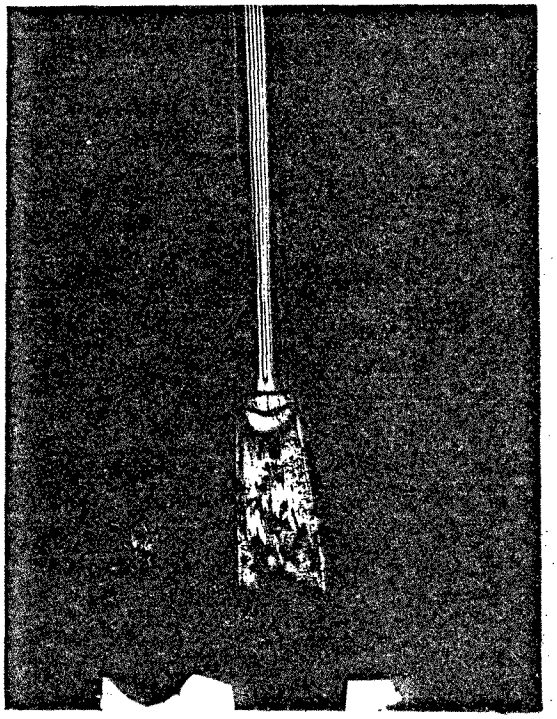

6D

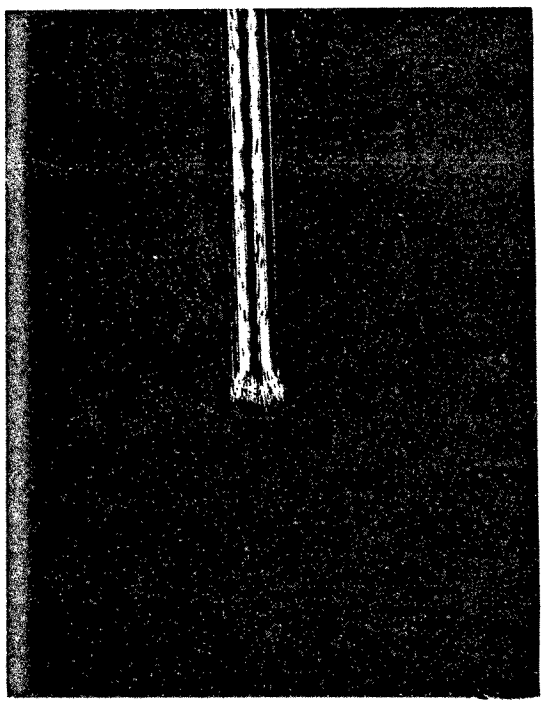

7A

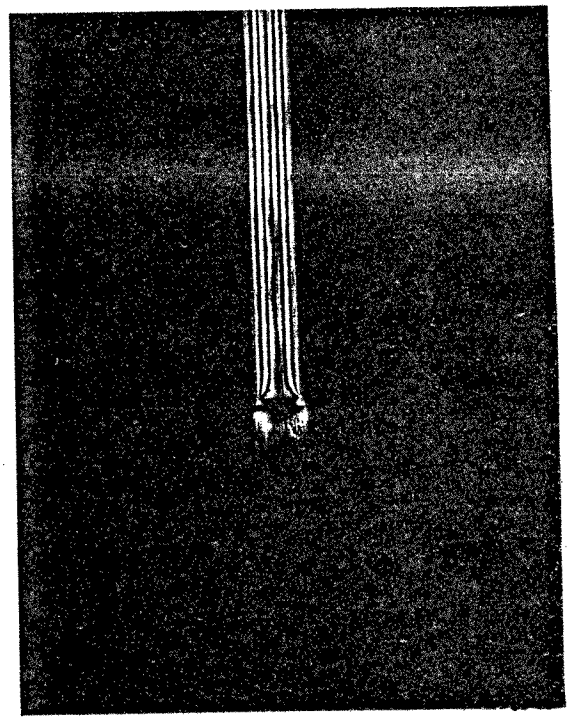

7B

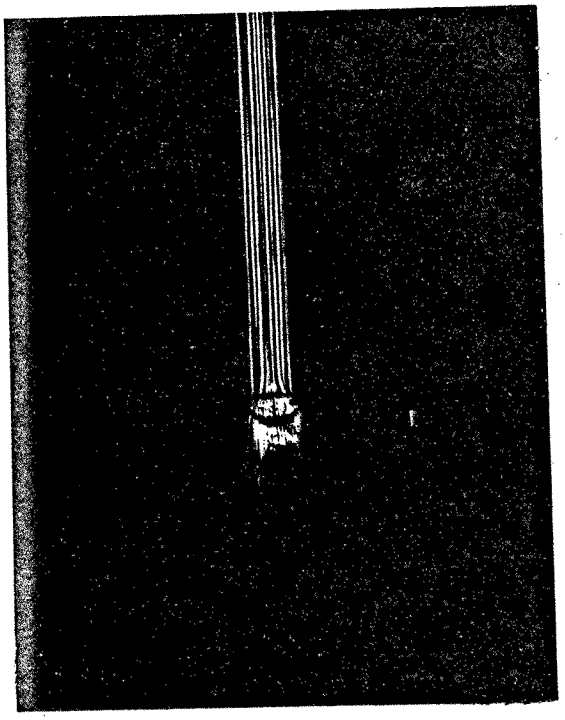

7C

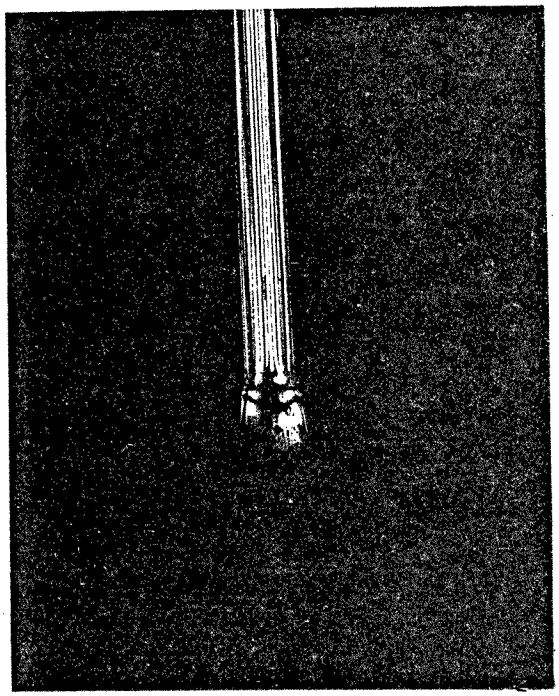

7D

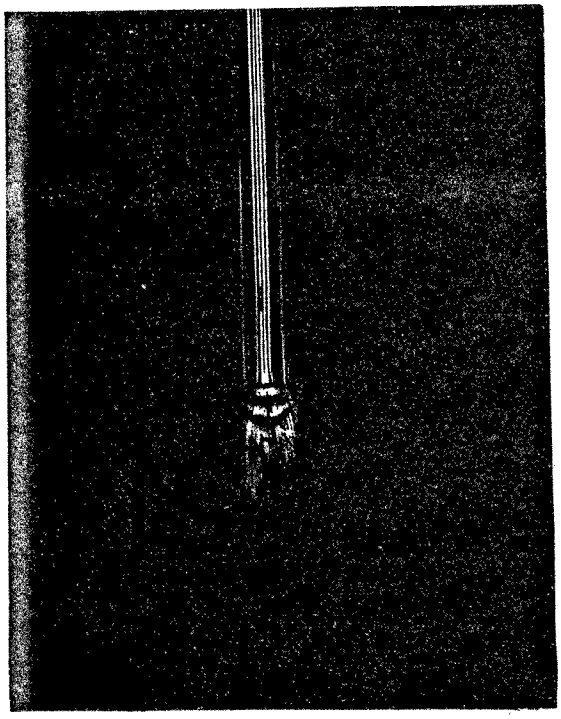

8A

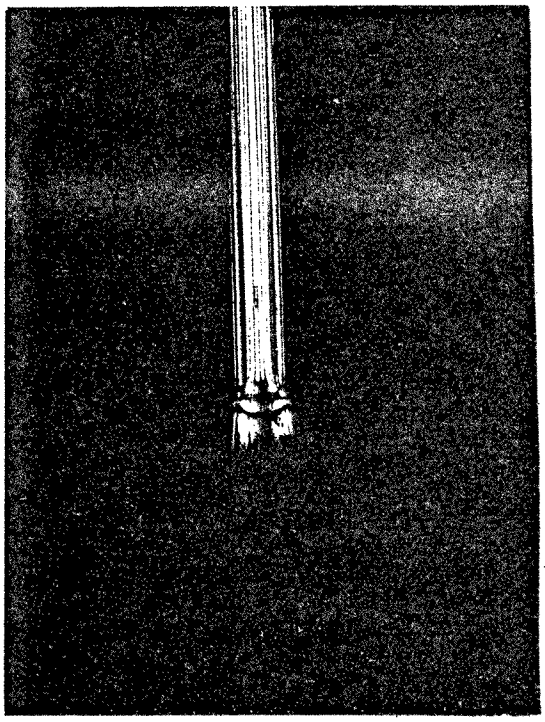

8B

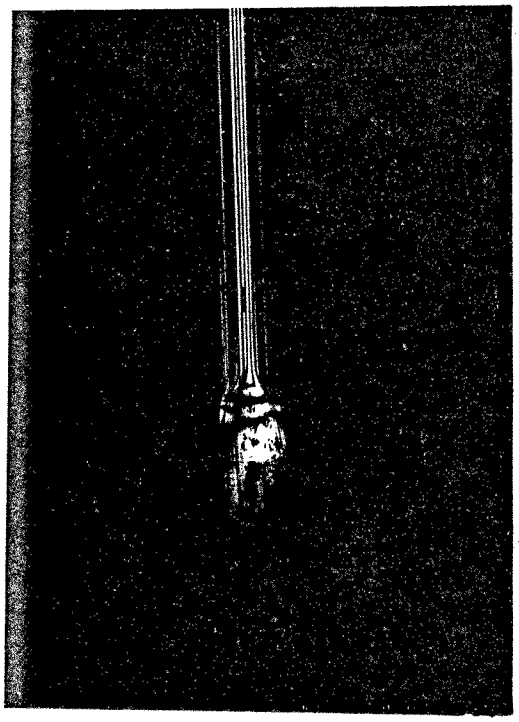

8C

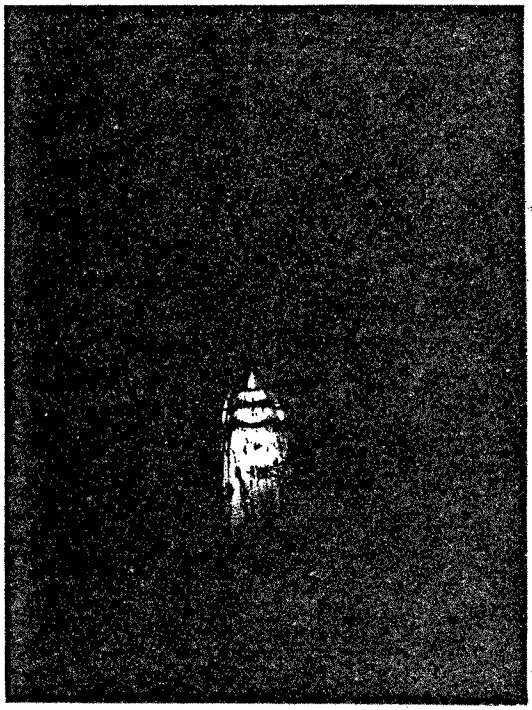

8D

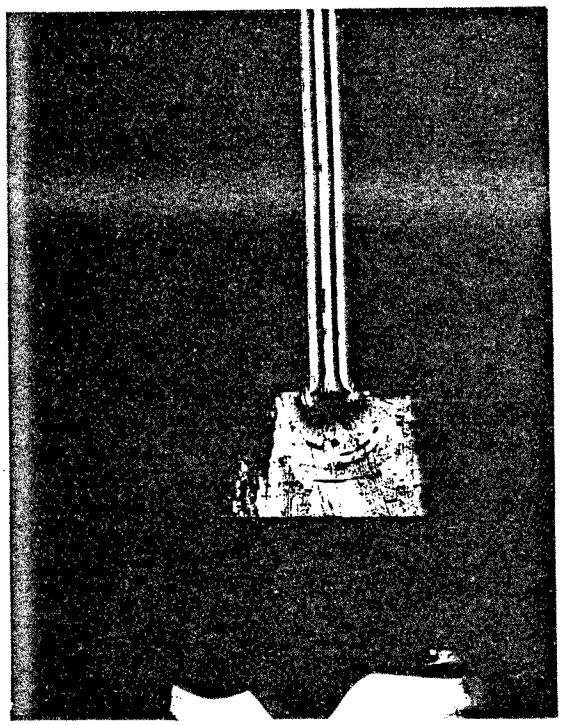

9A

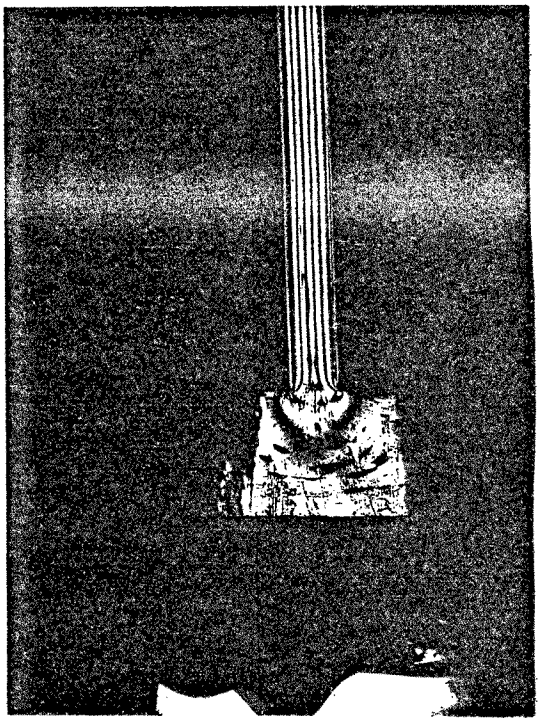

9B

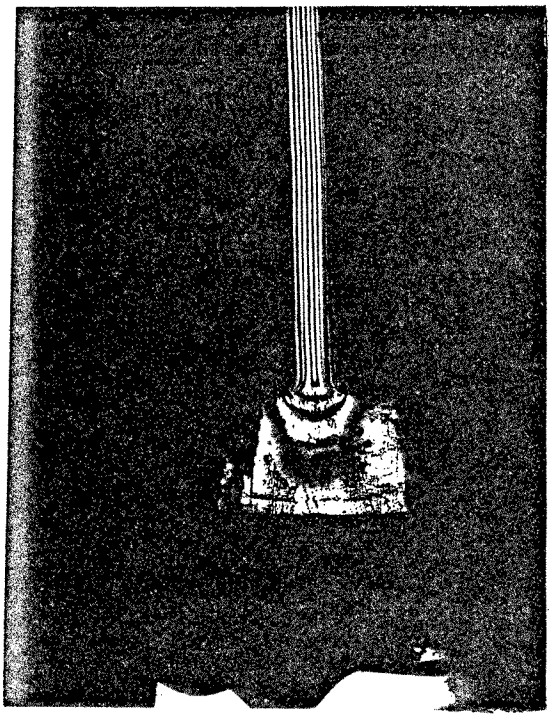

9C

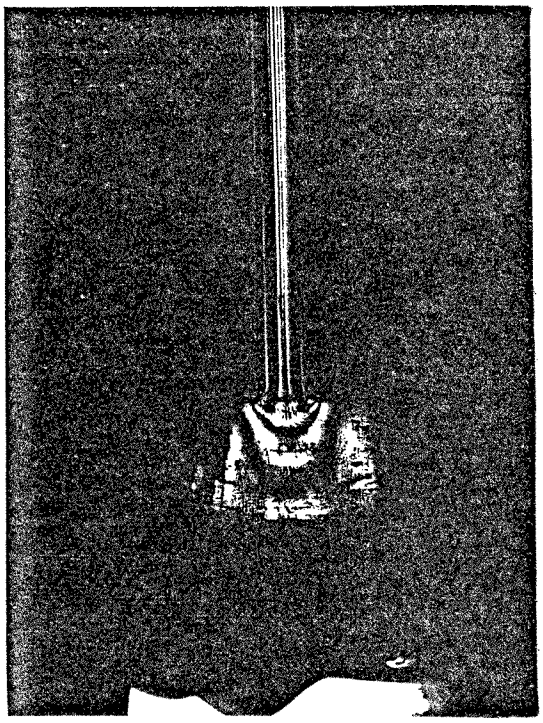

9D

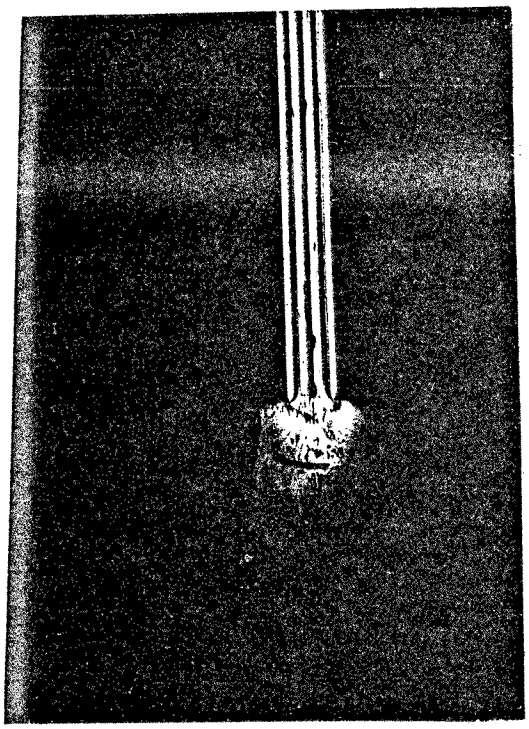

10A

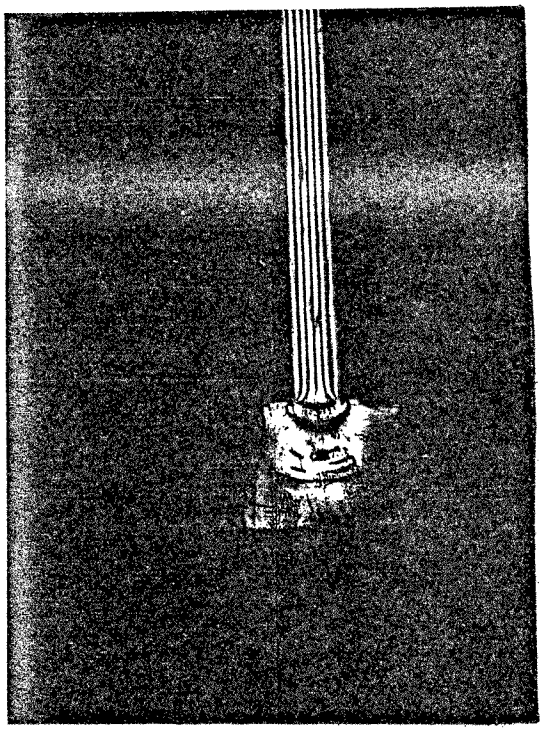

10B

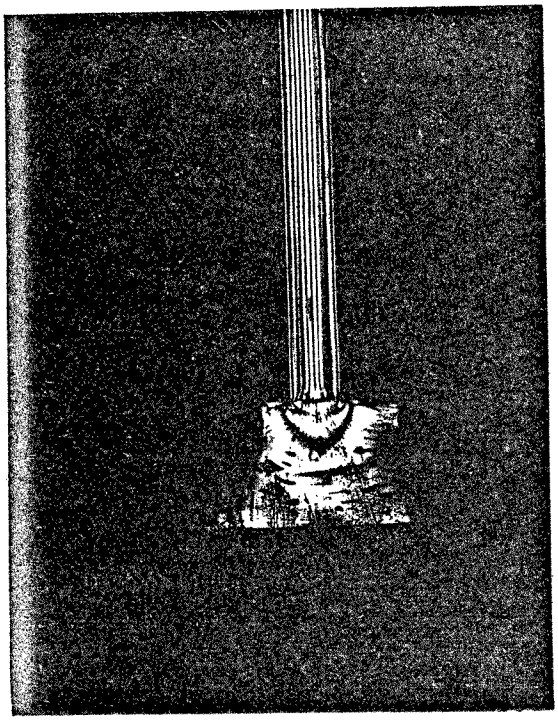

10C

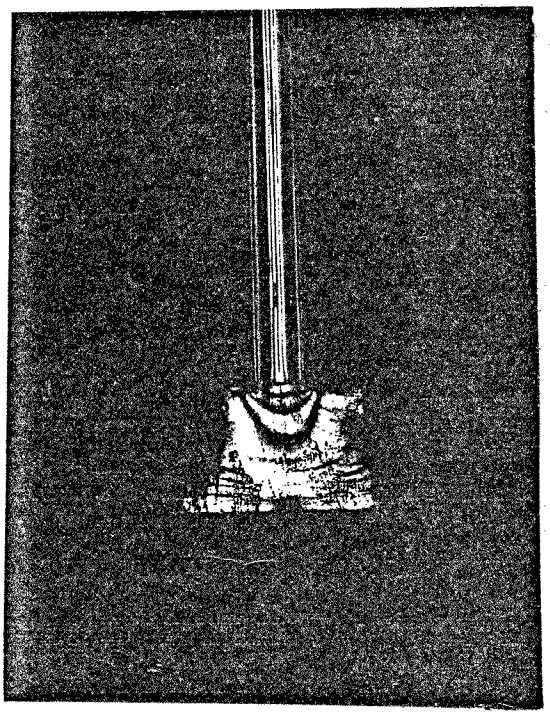

10D

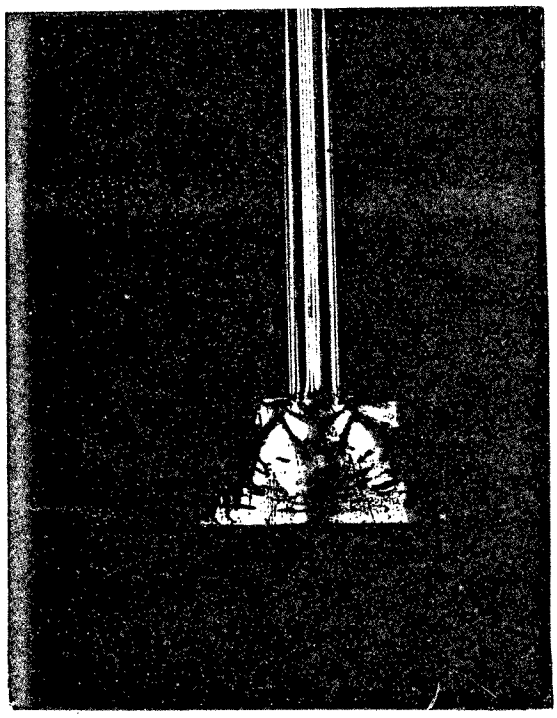

11A

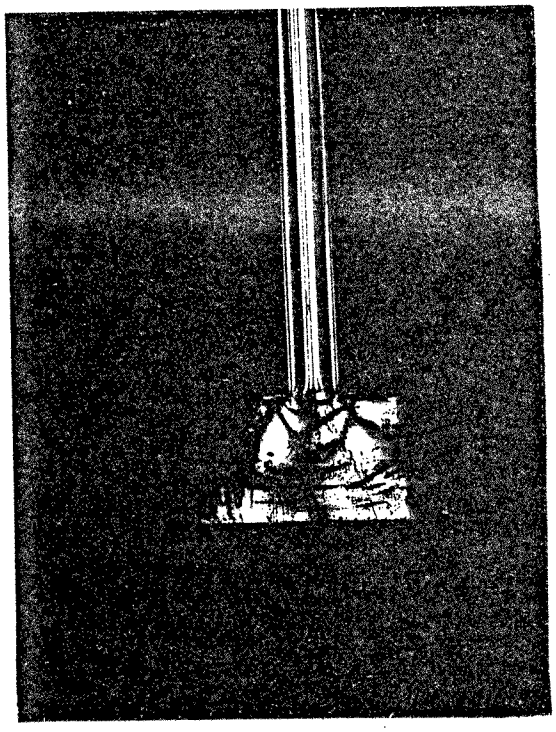

11B

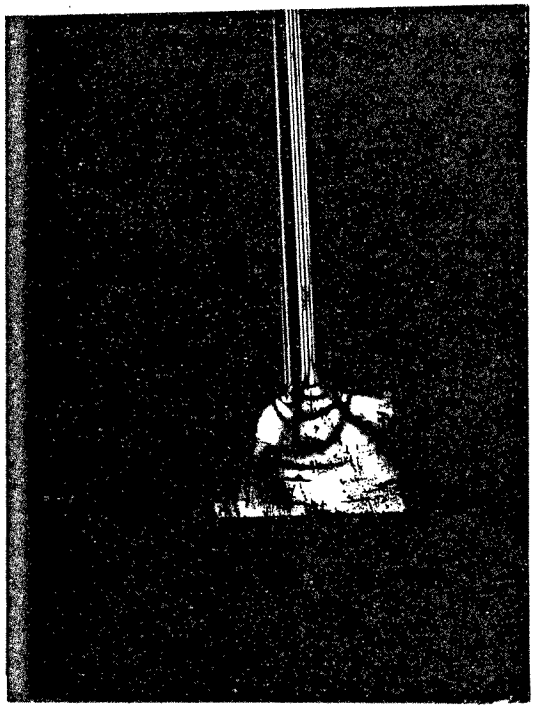

11C

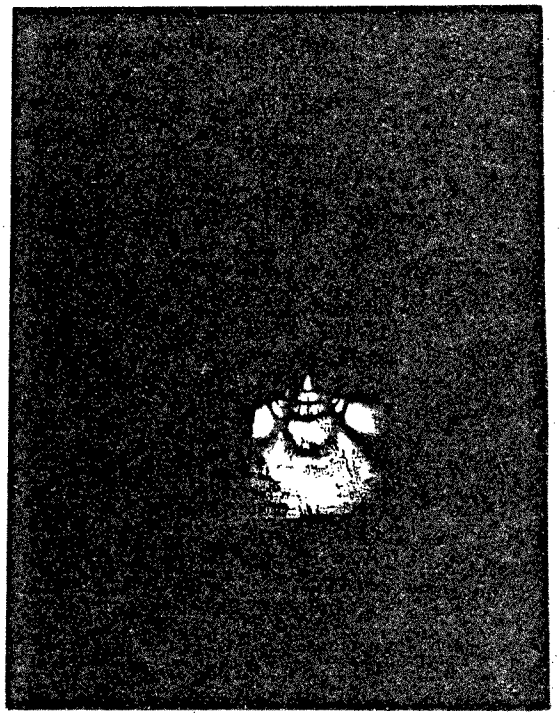

11D

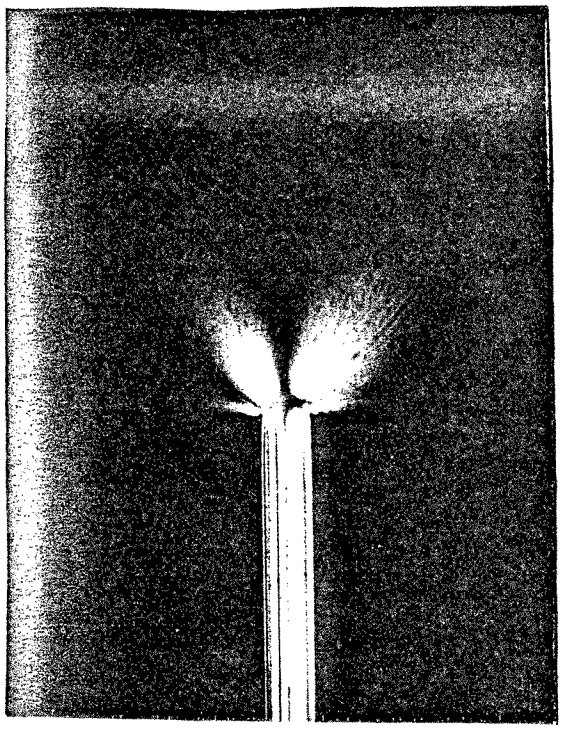

12 A

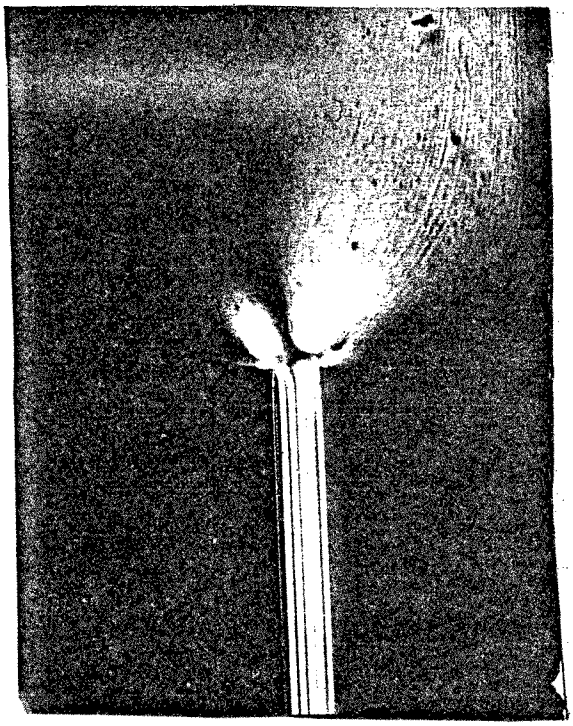

12 B

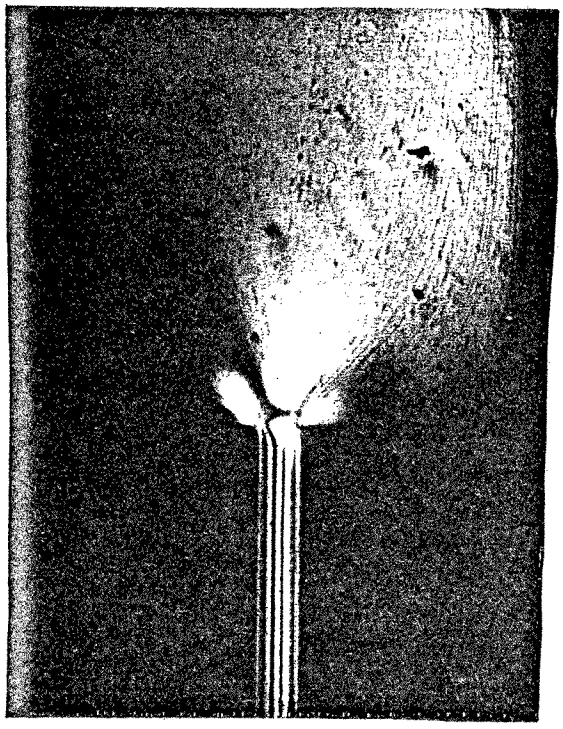

12 C

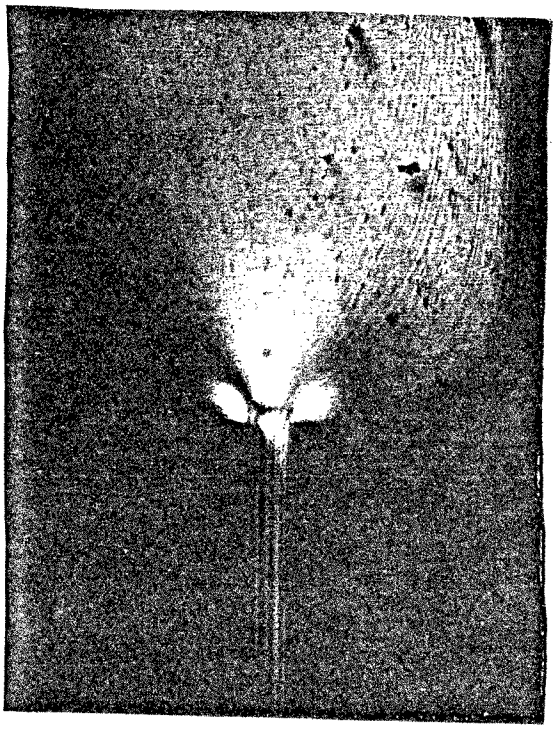

12 D

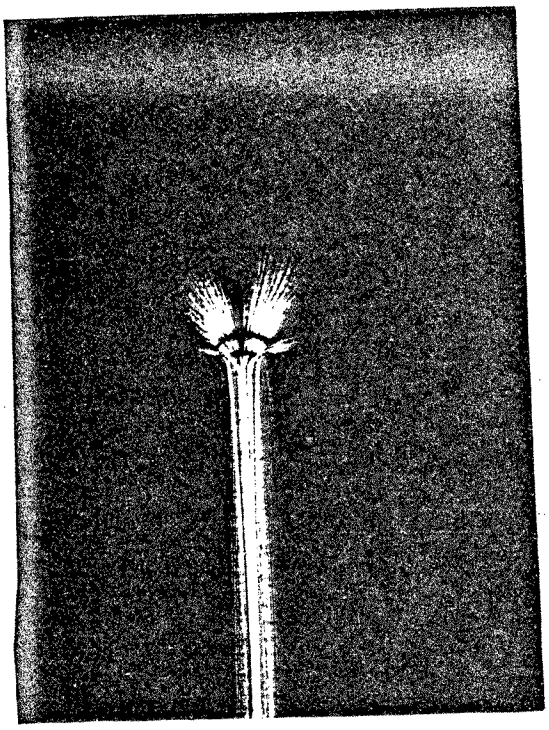

13A

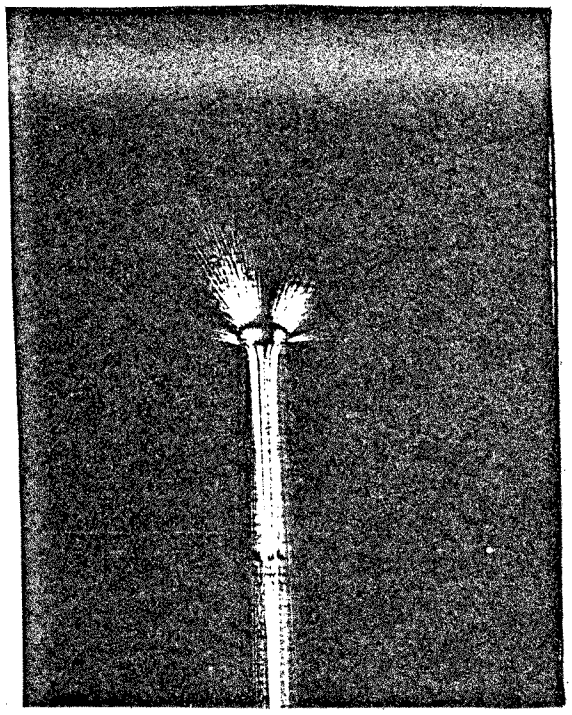

13B

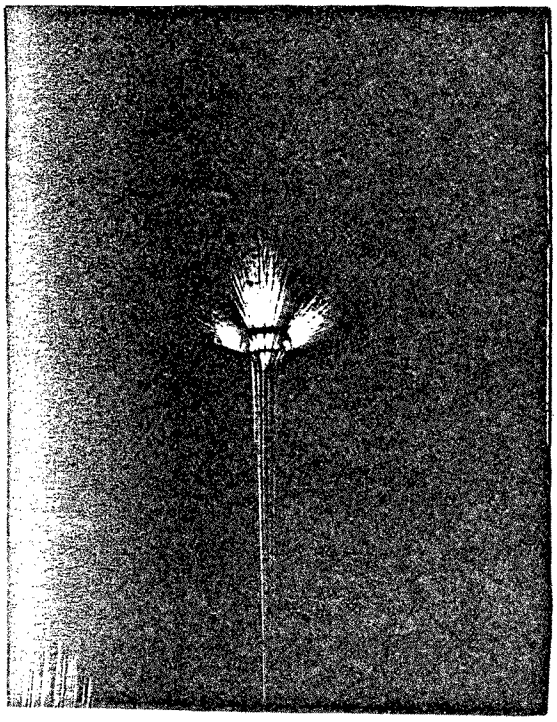

13C

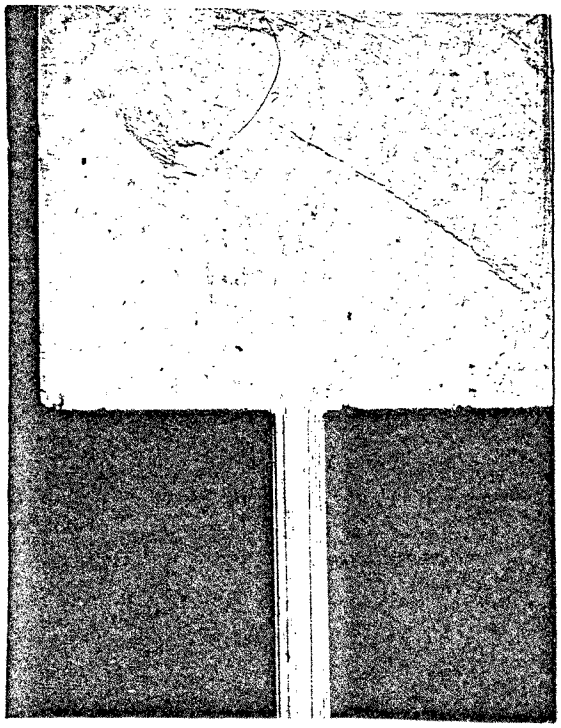

13D

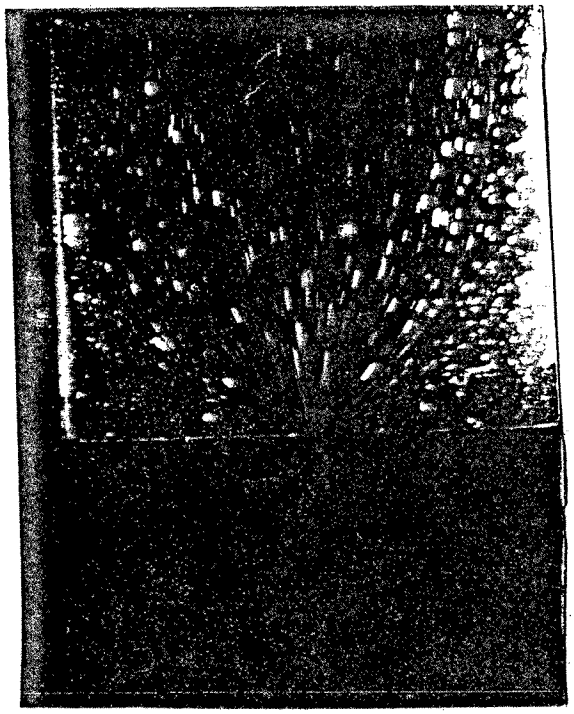

14A

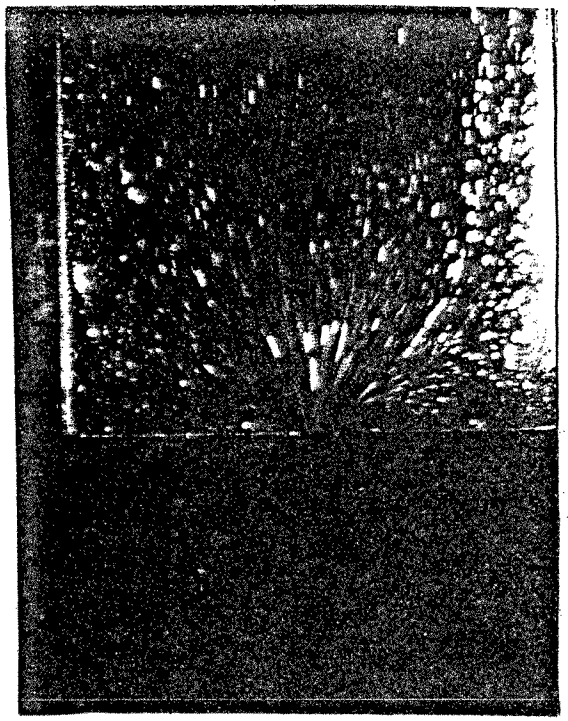

14B

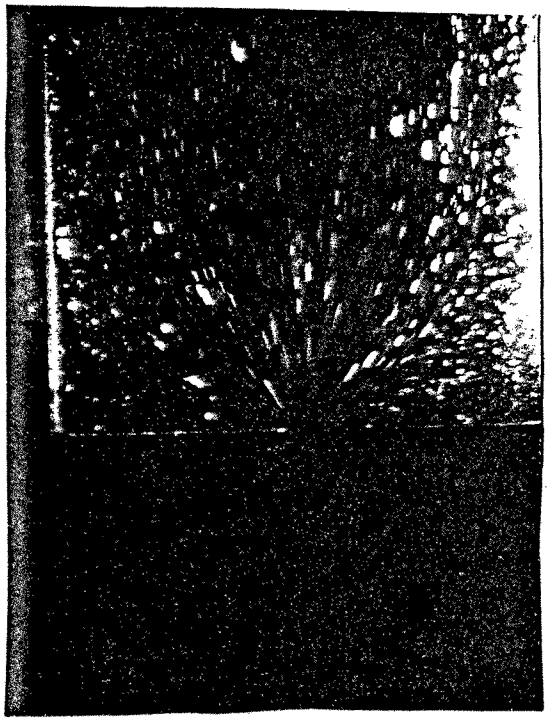

14C

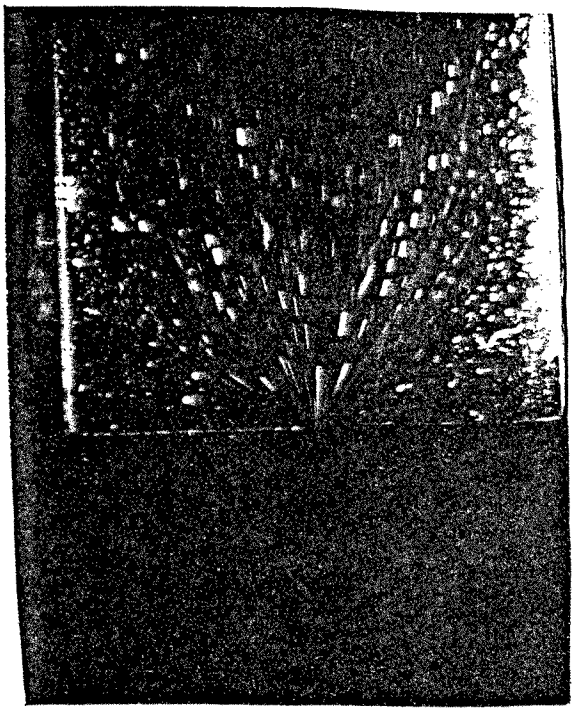

14D

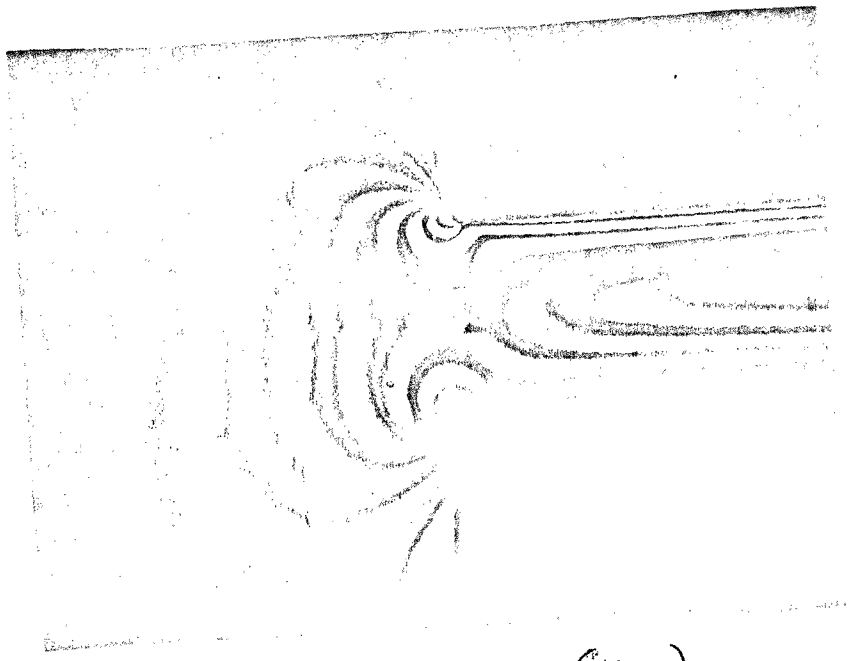

15a

Polypropylene (Mori)

$\tau = 420{,}000$ dynes/cm^2

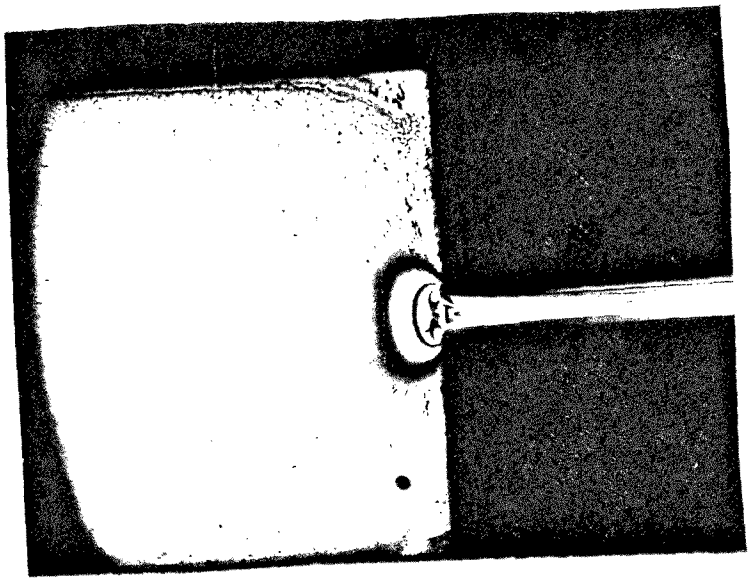

15b

Indopol H-1900

$\tau = 440{,}000$ dynes/cm^2

DISCUSSION OF RESULTS

Theory appears to hold within experimental accuracy for θ less than 60°. Beyond this point the effect of the slit width distorts the findings. From the pictures this area is bounded by the slit entrance plane and a semicircle of radius equal to half the slit width.

One of the items of particular interest was the stress pattern in the slit. For a newtonian material the difference of principal stresses in the slit should occur at an angle of 45 degrees. When the 45 degree isoclinic picture (8d) was evaluated in the slit region it showed a total absence of light in the slit proving the difference in principal stresses were indeed at 45°. Another finding that occurred as an outcrop of this is that the isochromatics in the slit which are parallel to each other are also equidistant (Graph 4).

In the entrance region the zero fringe order was found to move into the slit as the pressure was increased. Knowing the slit centerline velocity for each pressure it was found that the time it took the stress to degrade from its maximum to zero for every flow rate was a constant (Graph 7).

Putting the theoretical results in short form yields:

1) $r/r_o = \frac{1}{\sqrt{N}}$

2) $\alpha = 3/2\,\theta$

3) $V/V_c = \cos^{3/2}\theta$

All were found to hold true over a large range.

Also found:

4) The fringes in the slit are equidistant.

5) The difference in principal stress in the slit is at 45°.

6) The fringes in the slit are parallel to the walls and each other.

7) The zero fringe is centrally located in the slit in dark field and white light.

Fringe multiplication was found to be useful but was hampered by the size and sensitivity of the camera film. The technique of fringe sharpening however was entirely unsuccessful, probably due to the film being used which was low contrast in nature.

For the exit conditions the exit to air photographs yielded different patterns than the submerged exit and both exits differed from the entrance (pictures 2, 3, 6, 7, 9, 10, a through d). The main difference was that the "bun" in the entrance was tangent to the flat entry for large values of θ while the submerged exit showed the "bun" to intersect the flat at close to a right angle. Due to the nature of the exit to air the "buns" could not be evaluated in this region. The exit to air pictures, however, showed a faster stress degradation than the submerged exit.

The velocity pictures it was found could only be evaluated for low flow rates or the streak lengths would confuse the evaluation. Going to a shorter time it was feared would create an error in the time measurement significant enough to cancel the benefits of the high flow rate. It was found necessary to light only a central slice to eliminate end effects. This was unlike Han who in his experiments claimed the end effects could be averaged out.

In addition an unexplained effect was found that appears as an apparently optical convergence in the slit. The effect was proportional to the shear rate and was superimposed on the stress pattern without causing any change or discrepancy in the stress pattern (convergence is visible on pictures taken at 6.3, and 8.3 cc/sec i.e., $\tau = 3.34 \times 10^5$, 4.4×10^5 dynes/cm^2).

CONCLUSION

By stating that a material is newtonian you are in effect saying that the birefringence is linearly proportional to the stress. Under this assumption then, the fringes in the slit should be equidistant and this was proven to be true (Graph 4). Also the difference in principal stresses in the slit should be oriented at 45° this also was found to be true (8d).

Theoretical predictions in the slit and the entrance region were shown to hold true except in a region bounded by the slit entrance plane and a radius equal to half the slit width graphs of theoretical predictions illustrate this fact (Graph 6).

As regards comparison of newtonian and viscoelastic fluids three major differences are noted (see pictures 15a, 15b).

For the viscoelastic fluids the line of zero stress in the slit is located 5 to 14 slit widths into the slit. For comparable shear stresses the line of zero stress for the Indopol was within .2 slit widths of the entrance. The slit fringes were rounded on top for the viscoelastic fluid and almost square for the Indopol.

Viscoelastic fluids show stress concentrations at the corners of the slit entrance; the Indopol did not show any

at the lower shear stresses tested and was minimal at the higher range.

Indopol showed its "bun" shape profile throughout all the tests but the viscoelastic fluids show a higher radius at 45^{o} to the vertical. Again at higher shears the Indopol "bun" began to resemble that of the viscoelastic fluids.

The flow through inhomogenieties in the fluid was shown to be radial in the entrance region and became parallel almost immediately upon reaching the slit entrance plane.

The recommendations include a higher contrast film and greater optical magnification. This would allow for; better evaluation of isoclines, the application of fringe multiplication and fringe sharpening, and closer evaluation of stress concentrations.

Future investigations should include holographic stress evaluations, use of viscoelastic fluids, changes in entrance geometry, and changes in exit geometry. Further investigations into pressure and temperature profiles might also be warranted.

CALIBRATION OF FLUSH MOUNTED PRESSURE TRANSDUCER
TRANSDUCER IS MOUNTED DIRECTLY OPPOSITE THERMISTOR
44.9% LOSS IN SYSTEM
SHEAR STRESS 2 DYNES/CM² X 10⁻⁵
PRESSURE DROP ON SLIT PSI
FLUID RESERVOIR PRESSURE PSI
0
1
2
3
4
50
100
150
200
250
300
350
400

Graph 1

Graph 2

CALIBRATION OF LINEAR THERMISTOR

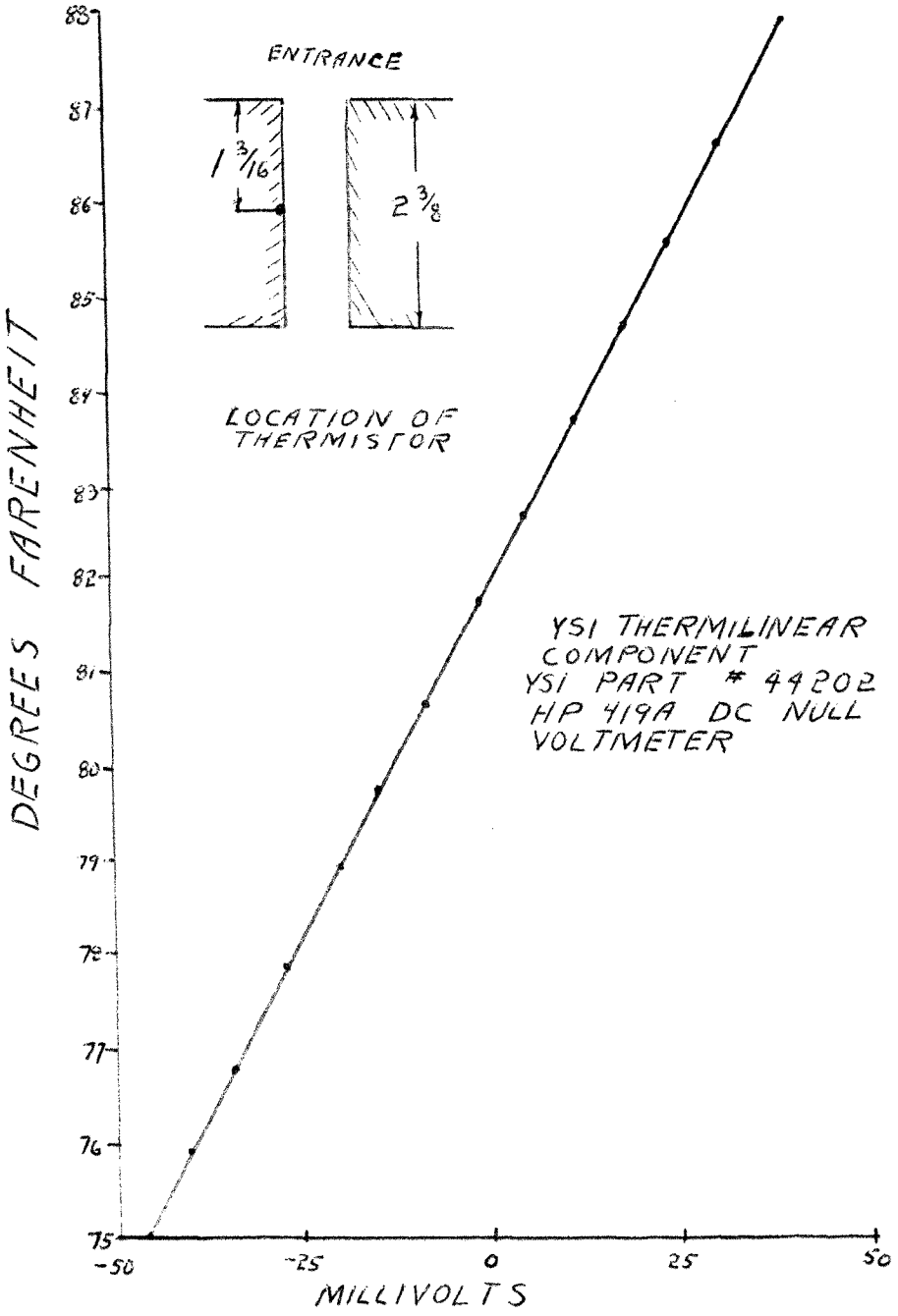

FIGURE 10

ENTRANCE ISOCLINIC AND ISOCHROMATIC PATTERN

Q = 8.3 cc/sec

$\tau = 4.40 \times 10^5$ dynes/cm^2

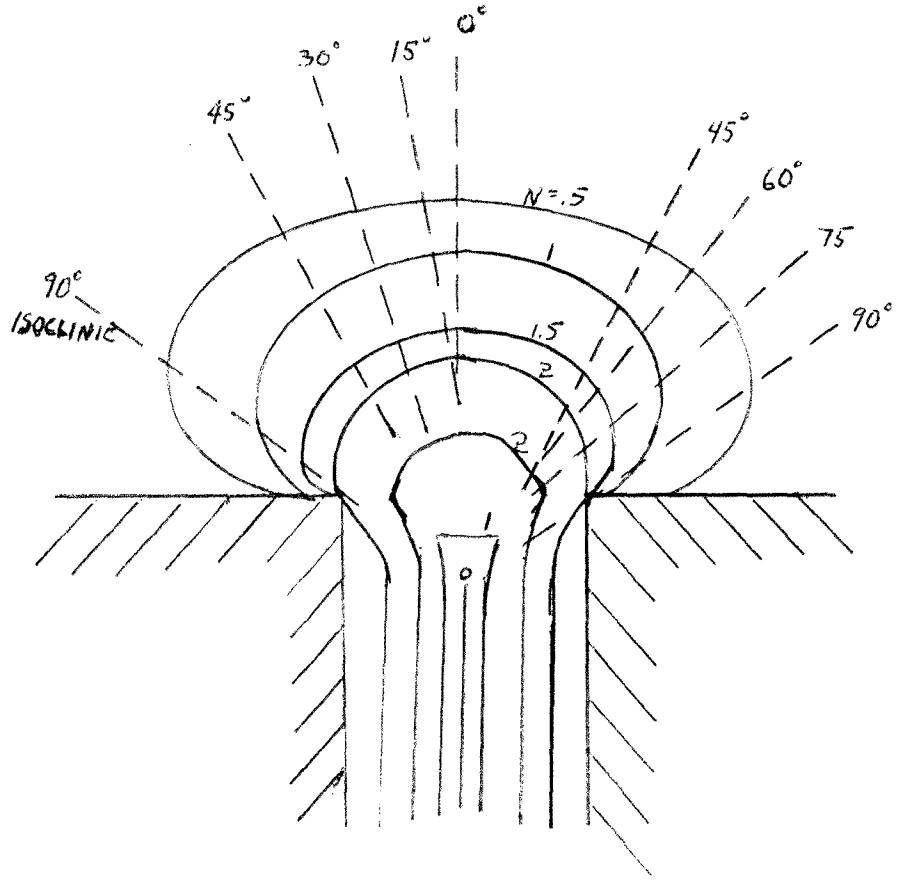

FIGURE 11

EXIT TO AIR ISOCLINIC AND ISOCHROMATIC PATTERN FOR

$Q = 8.3$ c.c/sec

$\Sigma = 4.40 \times 10^5$ dynes/cm^2

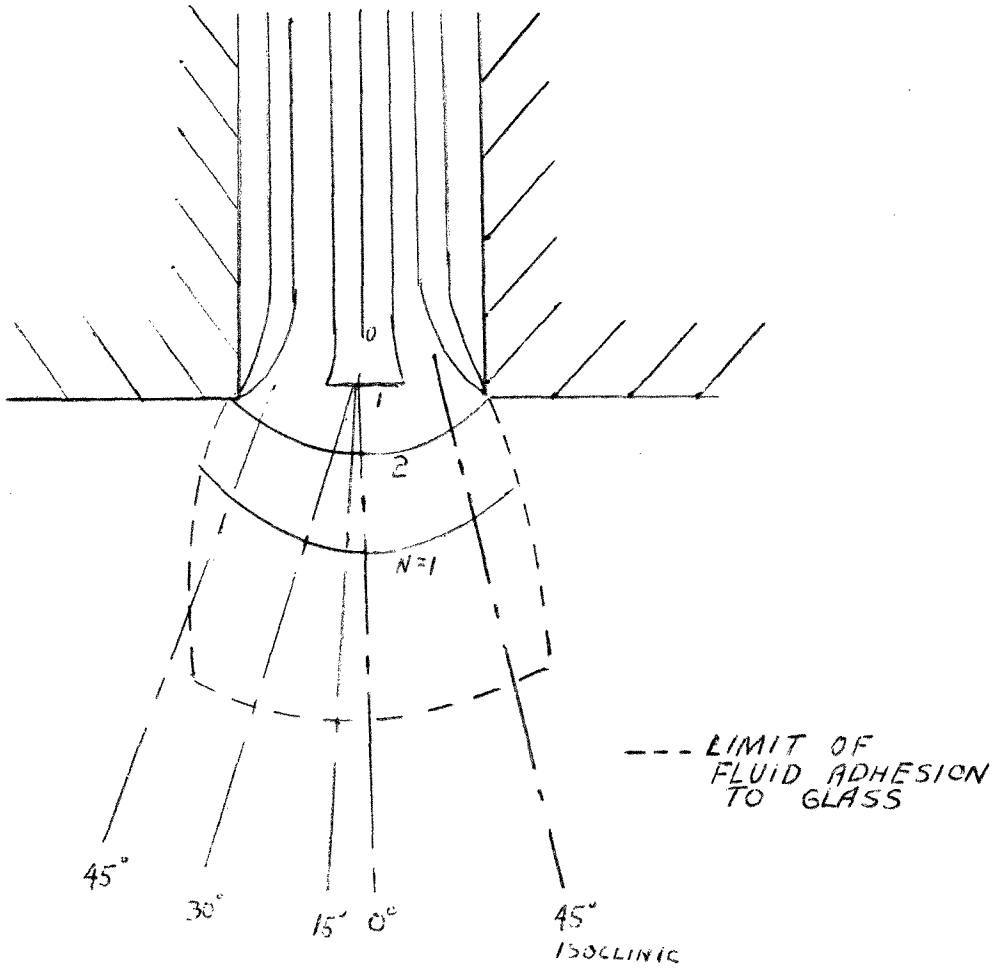

Figure 12

SUBMERGED EXIT ISOCLINIC AND ISOCHROMATIC PATTERN FOR

$Q = 8.3$ cc/sec

$\Sigma = 4.40 \times 10^5$ dynes/cm²

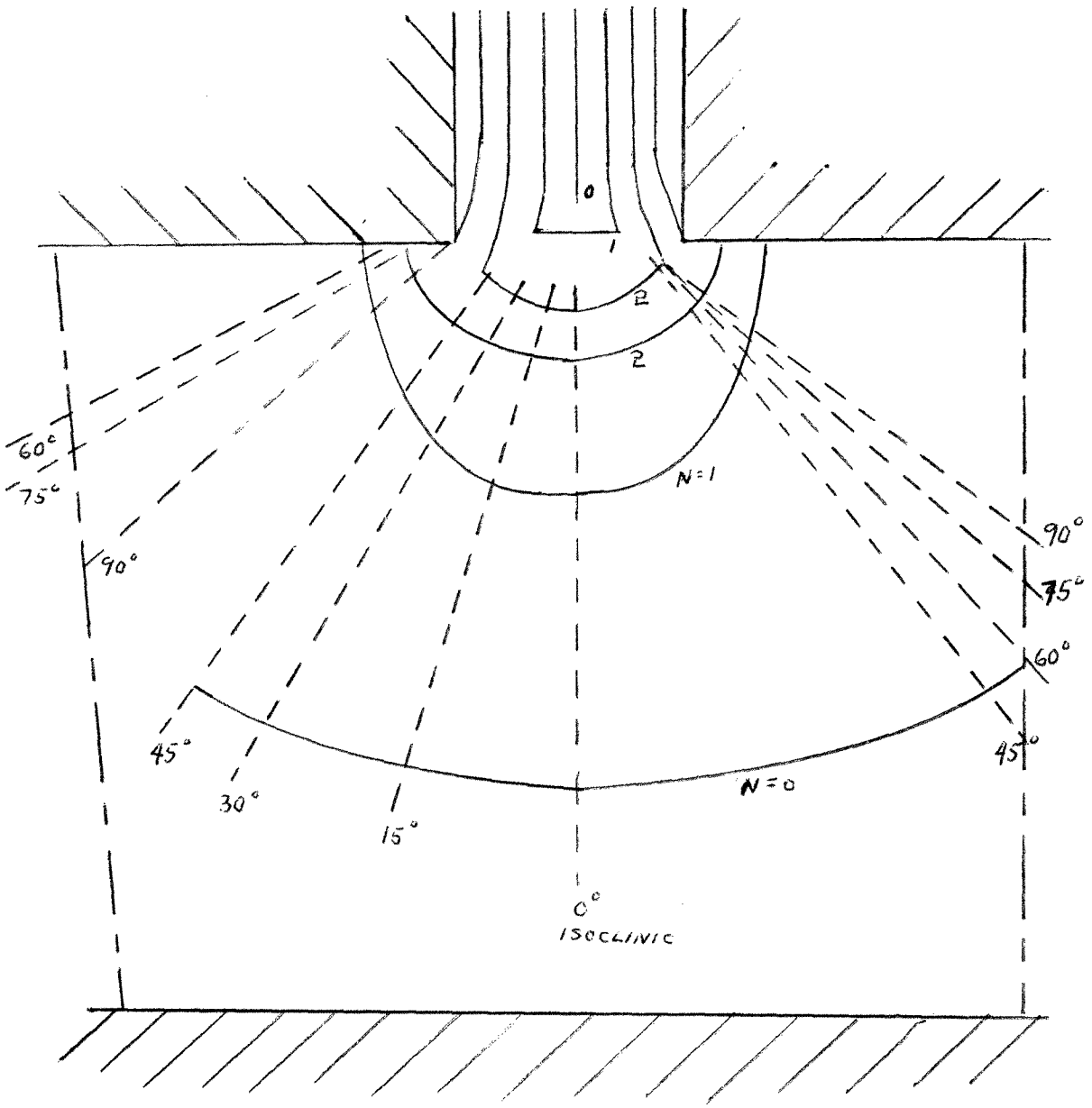

——— LIMIT OF FLUID ADHESION TO GLASS

FRINGE RADII

θ	N=.5	N=1	N=1.5	N=2
0	.403	.300	.189	.165
10	.389	.292	.199	.155
20	.406	.292	.202	.155
30	.415	.291	.203	.158
40	.430	.296	.214	.163
50	.425	.285	.211	.180
60	.425	.294	.238	.184
70	.375	.275	.223	.194
80	.325	.254	.213	.188
90	.225	.197	.183	.177

All radii values measured in centimeters

Angle is measured from vertical

Buns are symmetric about the vertical axis

USEFUL DATA ON BUN SHAPES

Data taken for 8.3cc/sec. N=.5 $Z = 4.4 \times 10^5$

Values in this table are relative to each other

A	H	H_2	A/H	H_2/H
34	19	10	1.78	.526
33	18	7	1.83	.388
33	19	7	1.73	.368
34	20	9	1.70	.450
36	20	11	1.80	.550
34	19	7	1.78	.368
34	20	9	1.70	.450
33	18	7	1.83	.388
31	20	8	1.55	.400
31	21	9	1.55	.428
31	21	9	1.55	.428
33.09	19.54	8.45	1.71	.432

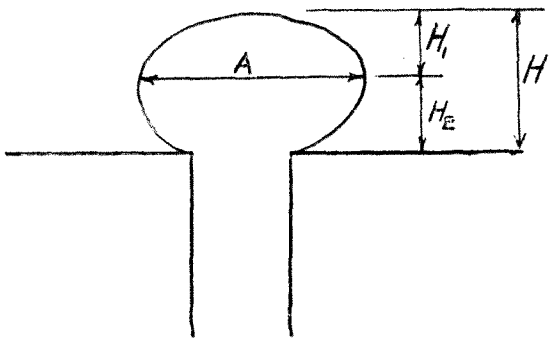

USEFUL DATA ON BUN SHAPES

Data taken for 8.3cc/sec. N=1 $Z = 4.4 \times 10^{5}$

Values in this table are relative to each other

A	H	H_2	A/H	H_2/H
24	13	5	1.84	.386
24	12.5	6	1.92	.480
23.5	13.5	6	1.67	.444
24.5	14	5.5	1.75	.407
23.5	13.5	4.5	1.74	.333
23.5	13.5	5.5	1.74	.407
24	13.5	5	1.77	.370
24.5	14.5	6	1.68	.413
23.9	13.5	5.4	1.76	.405

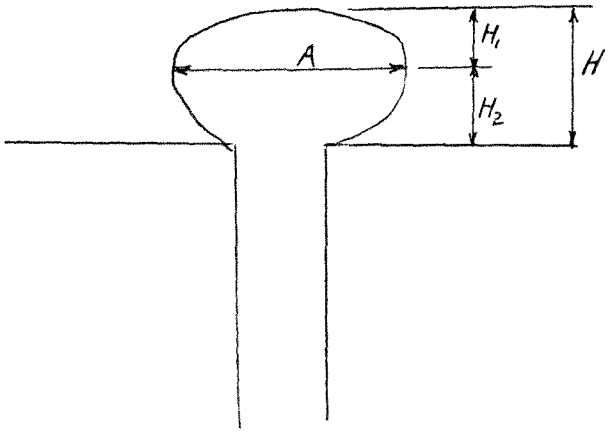

USEFUL DATA ON BUN SHAPES

Data taken for 8.3cc/sec. N=1.5 $\nu = 4.4 \times 10^{-5}$

Values in this table are relative to each other

A	H	H_2	A/H	H_2/H
22	10	5	2.20	.500
21	11	4	1.91	.364
21	10	4	2.10	.400
22	11	5	2.00	.454
21	9	4	2.33	.444
22	9	4	2.44	.444
21	10	6	2.10	.600
21	9	4	2.44	.444
20	10	3	2.00	.300
20	10	5	2.00	.500
20	11	6	1.81	.545
21	10	4.7	2.12	.454

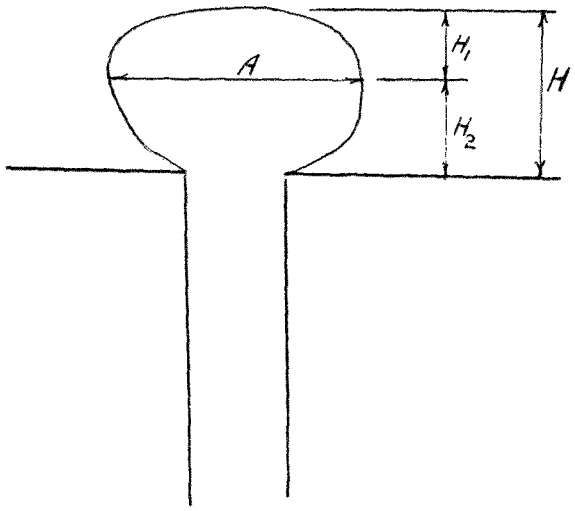

ISOCLINES

Entrance	Polarization Angle	Isoclinic angle to vertical
8.3cc/sec. $\tau = 4.4 \times 10^{-5}$	0	0
	15	10
	30	18
	45	28,28
	60	47.5
	75	48.5
	90	53.5,55.5
Exit (air)	0	1
8.3cc/sec. $\tau = 4.4 \times 10^{-5}$	15	4.5
	30	17.5
	45	14,20.5
	60	—
	75	—
	90	—
Exit (submerged)	0	0
8.3cc/sec. $\tau = 4.4 \times 10^{-5}$	15	16.5
	30	30.5
	45	36.5,35
	60	39.5,42
	75	45.5,56
	90	50,48

ENTRANCE ISOCLINES

α	θ(3.1 cc/sec)	θ(4.2 cc/sec)	θ(8.3 cc/sec)
0	0	0	0
15	11,10	—	10
22.5	—	16	—
30	20,20	—	20
45	31,30,30	30,30	29,29
60	39,40	—	38.5
67.5	—	45.5	—
75	51,50,50	—	49
90	60,60	61,60	58.5,59

All readings in degrees.

α = Angle of polarization

θ = Isoclinic angle to vertical

GRAPH 3

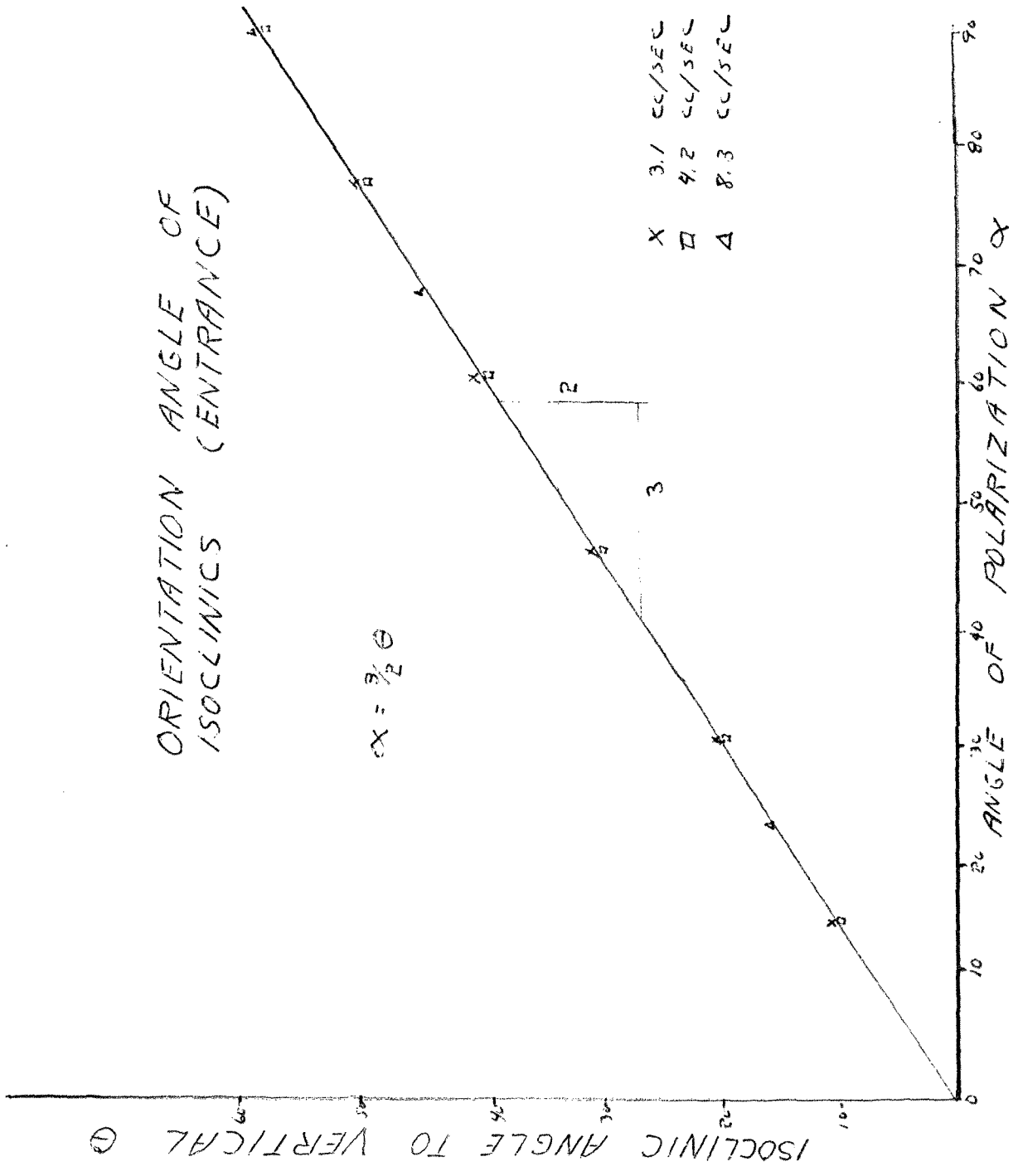
ORIENTATION ANGLE OF ISOCLINICS (ENTRANCE)
$\alpha = \frac{3}{2}\theta$
3
2
X 3.1 cc/sec
□ 4.2 cc/sec
Δ 8.3 cc/sec
ISOCLINIC ANGLE TO VERTICAL θ
ANGLE OF POLARIZATION α
0
10
20
30
40
50
60
70
80
90

ENTRANCE FRINGE SEQUENCES

(polyethylene)

Author: Han								Author: Mori		
$\bar{z}$ = 5×10^5		$\bar{z}$ = 3.6×10^5		$\bar{z}$ = 3.2×10^5		$\bar{z}$ = 2.5×10^5		$\bar{z}$ = 3.5×10^5		
N/N_0	x/b	N/N_0	x/b	N/N_0	x/b	N/N_0	x/b	N/N_0	x/b	
.16	—							.153	2.67	
.38	4.5							.307	1.79	
.5	1.8							.461	1.29	Slit side
.61	1	.5	2.85					.615	.970	
.72	.53	.64	.952	.5	2	.55	2.85	.769	.676	
.83	.28	.78	.6	.7	.76	.77	.33	.92	.324	
.94	0	.92	.238	.9	.284	.88	.23	1	.148	
1	.19	1	.04	1	.142	1	0	.92	.029	
.94	.38	.92	.33	.9	.619	.88	.23	.769	.324	
.83	.57	.78	.57	.7	1.09	.77	.33	.615	.558	
.72	.76	.64	.904	.5	1.71	.55	.714	.461	.912	
.61	.95	.5	1.38	.3	2.85	.33	1.28	.307	1.67	Reservoir side
.5	1.28	.357	2.14	.1	6.09	.11	3.23	.153	4.7	
.38	1.8	.214	4.19							
.16	2.66									

ENTRANCE FRINGE SEQUENCE

(polypropylene)

Author: Han $Z =$ 3.8×10^5			Author: Mori $Z =$ 4.3×10^5	
N/N_o	x/b		N/N_o	x/b
.166	3.38		.444	.640
.5	.838	Slit	.666	.661
.833	.193	side	.888	.203
1	.022		1	.045
.833	.236		.888	.356
.5	.773	Reservoir	.666	.746
.166	1.97	side	.444	1.2
			.222	2.17

ENTRANCE FRINGE SEQUENCE

(Indopol H-1900)

Author: NCE

$\mathcal{Z}=4.4\times10^5$		$\mathcal{Z}=3.34\times10^5$		$\mathcal{Z}=2.23\times10^5$		$\mathcal{Z}=1.12\times10^5$	
N/N_o	x/b	N/N_o	x/b	N/N_o	x/b	N/N_o	x/b
0	.433	0	.396		Slit side		
.2	.306	.2	.181				
.4	.142	.4	.033	0	.356		
.6	.112	.6	.142	.33	.148	0	1.62
.8	.059	.8	.377	.66	.077	.5	.538
1	.223	1	.615	1	.265	1	.418
.8	.467	.8	.82	.66	.511	.833	.138
.6	.618	.6	1.07	.33	.987	.5	.022
.4	.943	.4	2.05	0	2.219	0	.442
.2	1.305	.2	3.89				
0	3.505				Reservoir side		

CENTERLINE FRINGE SEQUENCE

2.1cc/sec.
$\tau = 1.11 \times 10^5$ dynes/cm^2

Fringe Number	x/b
0	.442
$\frac{1}{6}$	-.022
5/6	-.138
1	-.418
$\frac{1}{2}$	-.538
0	-1.62

Positive value indicates fringe is located within the slit

Negative value indicates the fringe is located within the reservoir

CENTERLINE FRINGE SEQUENCE

4.2cc/sec.
$\tau = 2.23 \times 10^5$ dynes/cm^2

Fringe Number	x/b
0	.356
$\frac{1}{2}$	.148
1	-.077
$1\frac{1}{2}$	-.265
1	-.511
$\frac{1}{2}$	-.987
0	-2.219

Positive value indicates fringe is located within the slit.

Negative value indicates fringe is located within the reservoir.

CENTERLINE FRINGE SEQUENCE

6.3cc/sec.
$\tau = 3.34 \times 10^5$ dynes/cm^2

Fringe Number	x/b
0	.396
$\frac{1}{2}$	.265
1	-.035
$1\frac{1}{2}$	-.105
$1\frac{1}{2}$	-.252
1	-.578
$\frac{1}{2}$	-.997
0	-3.89

Negative sign indicates the fringe is located within the reservoir

Positive value indicates the fringe is located within the slit.

CENTERLINE FRINGE SEQUENCE

8.3cc/sec.
$\tau = 4.40 \times 10^5$ dynes/cm^2

Fringe Number	x/b
0	.433
$\frac{1}{5}$	.306
1	.141
$1\frac{1}{5}$	.112
2	-.059
$2\frac{1}{5}$	-.223
2	-.467
$1\frac{1}{5}$	-.618
1	-.943
$\frac{1}{5}$	-1.305
0	-3.505

Negative value indicates fringe is located within the reservoir.

Positive value indicates the fringe is located within the slit.

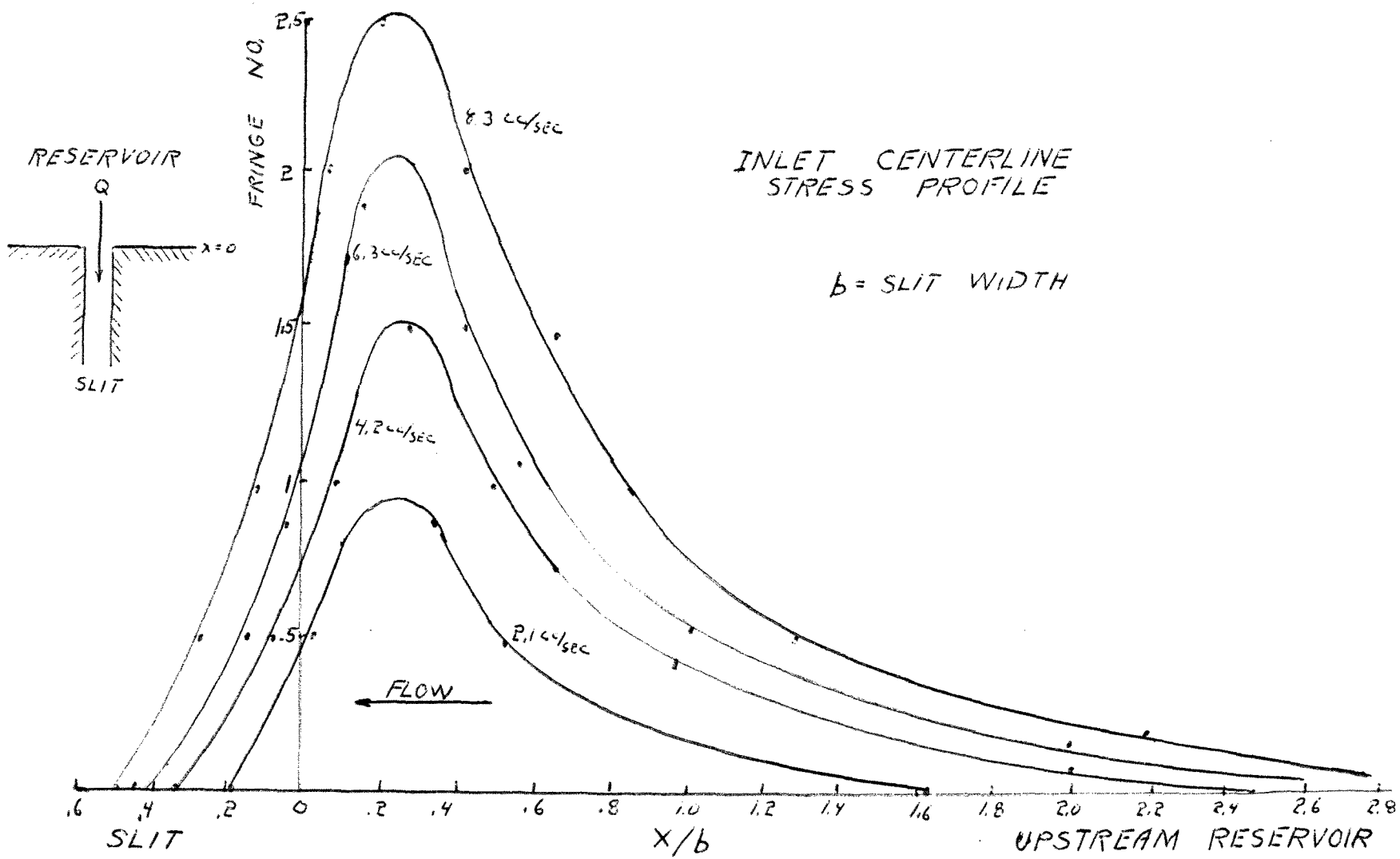
INLET CENTERLINE
STRESS PROFILE
b = SLIT WIDTH
RESERVOIR
Q
x = 0
SLIT
FRINGE NO.
2.5
2
1.5
1
.5
8.3 cc/sec
6.3 cc/sec
4.2 cc/sec
2.1 cc/sec
FLOW
.6
.4
.2
0
.2
.4
.6
.8
1.0
1.2
1.4
1.6
1.8
2.0
2.2
2.4
2.6
2.8
SLIT
X/b
UPSTREAM RESERVOIR

Figure 10

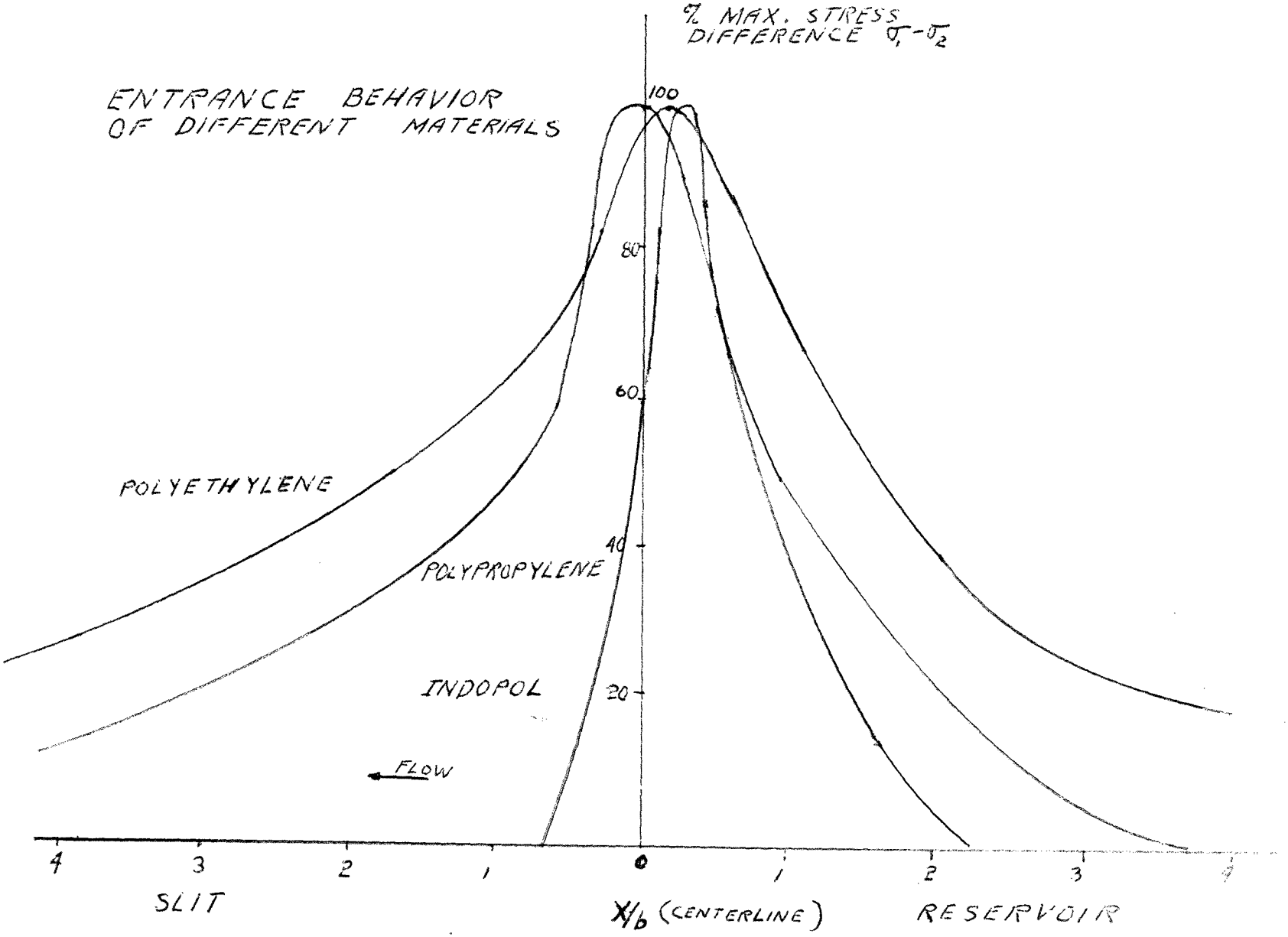
% MAX. STRESS DIFFERENCE $\sigma_1 - \sigma_2$
ENTRANCE BEHAVIOR OF DIFFERENT MATERIALS
100
80
60
40
20
POLYETHYLENE
POLYPROPYLENE
INDOPOL
FLOW
4
3
2
1
0
1
2
3
4
SLIT
X/b (CENTERLINE)
RESERVOIR

EXIT (AIR) CENTERLINE FRINGE SEQUENCE

Fringe Number	2.1 cc/sec. $\Sigma = (1.11 \times 10^{-5})$	4.2 cc/sec. (2.23×10^{-5})	6.3 cc/sec. (3.34×10^{-5})	8.3 cc/sec. (4.40×10^{-5})
0	.255	.340	.510	.510
$\frac{1}{5}$	-.085	.085	.425	.255
1	———	-.085	.170	.170
$1\frac{1}{5}$	———	———	-.085	-.085
$1\frac{1}{5}$	———	———	-.170	-.425
1	———	-.425	-.425	-.680
$\frac{1}{5}$	———	-.595	-.765	-.935
0	-.425	-1.1059	-1.276	-1.616

Tabulated values are that of x/b.

Positive values indicate the fringe is located within the slit.

Negative values indicate the fringe is located in the cell exit region.

EXIT (SUBMERGED) CENTERLINE FRINGE SEQUENCE

Fringe Number	2.1 cc/sec. $Z = (1.11 \times 10^{-3})$	4.2 cc/sec. (2.23×10^{-3})	6.3 cc/sec. (3.34×10^{-3})	8.3 cc/sec. (4.40×10^{-3})
0	.085	.255	.255	.425
$\frac{1}{2}$	-.085	.170	.170	.170
1	———	-.085	-.085	.085
$1\frac{1}{2}$	———	———	-.170	-.085
2	———	———	———	-.170
2	———	———	———	-.510
$1\frac{1}{2}$	———	———	-.595	-.850
1	———	-.595	-.935	-1.276
$\frac{1}{2}$	-.425	-.935	-1.701	-2.042
0	-2.467	-2.637	-2.807	-3.062

Tabulated values are that of x/b.

Positive values indicate fringe is located within the slit.

Negative values indicate the fringe is located in the exit reservoir.

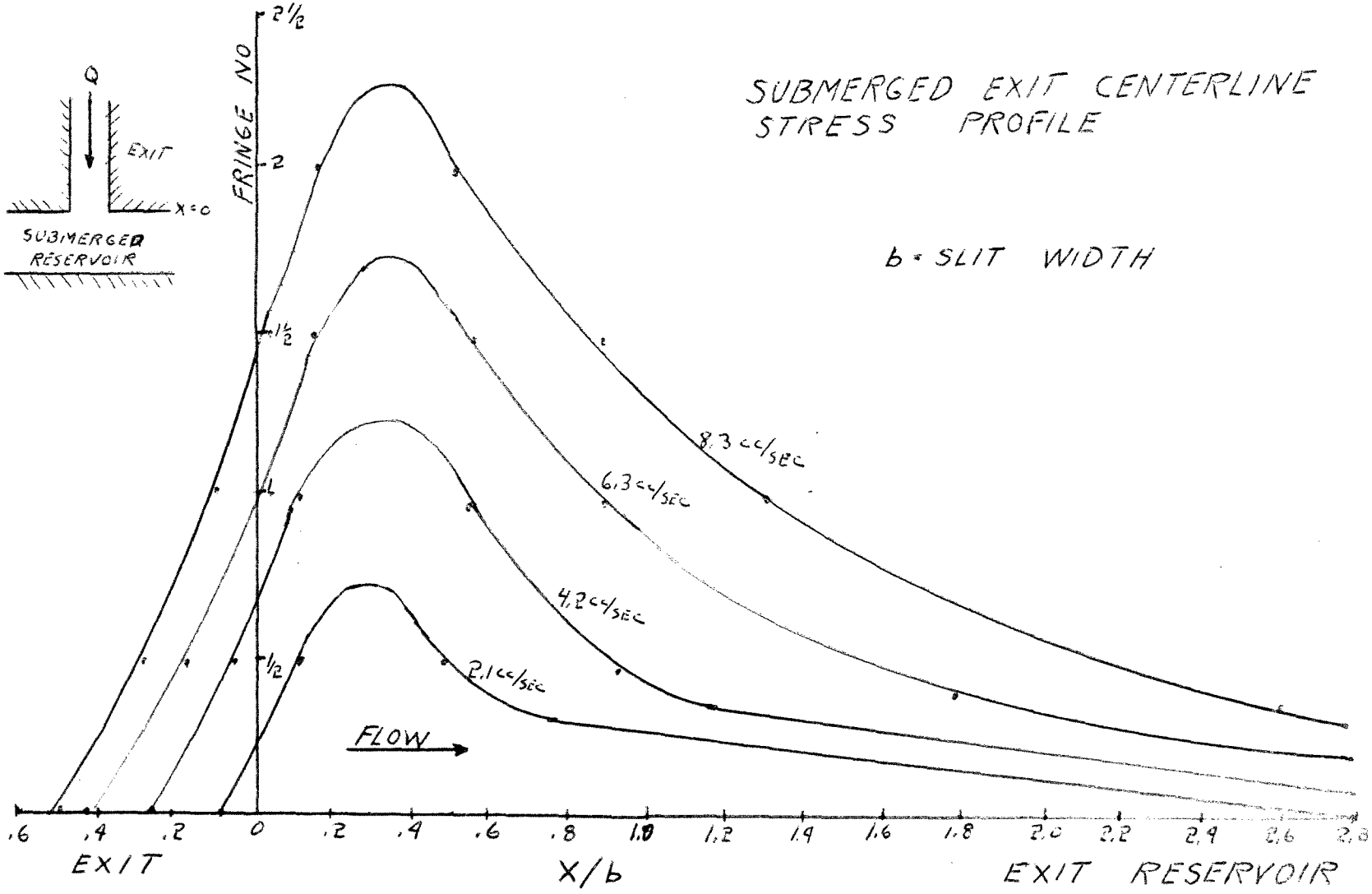
SUBMERGED EXIT CENTERLINE
STRESS PROFILE
b = SLIT WIDTH
Q
EXIT
X=0
SUBMERGED
RESERVOIR
FRINGE NO
2 1/2
2
1 1/2
1
1/2
8.3 cc/sec
6.3 cc/sec
4.2 cc/sec
2.1 cc/sec
FLOW
.6
.4
.2
0
.2
.4
.6
.8
1.0
1.2
1.4
1.6
1.8
2.0
2.2
2.4
2.6
2.8
EXIT
X/b
EXIT RESERVOIR

FIGURE 12

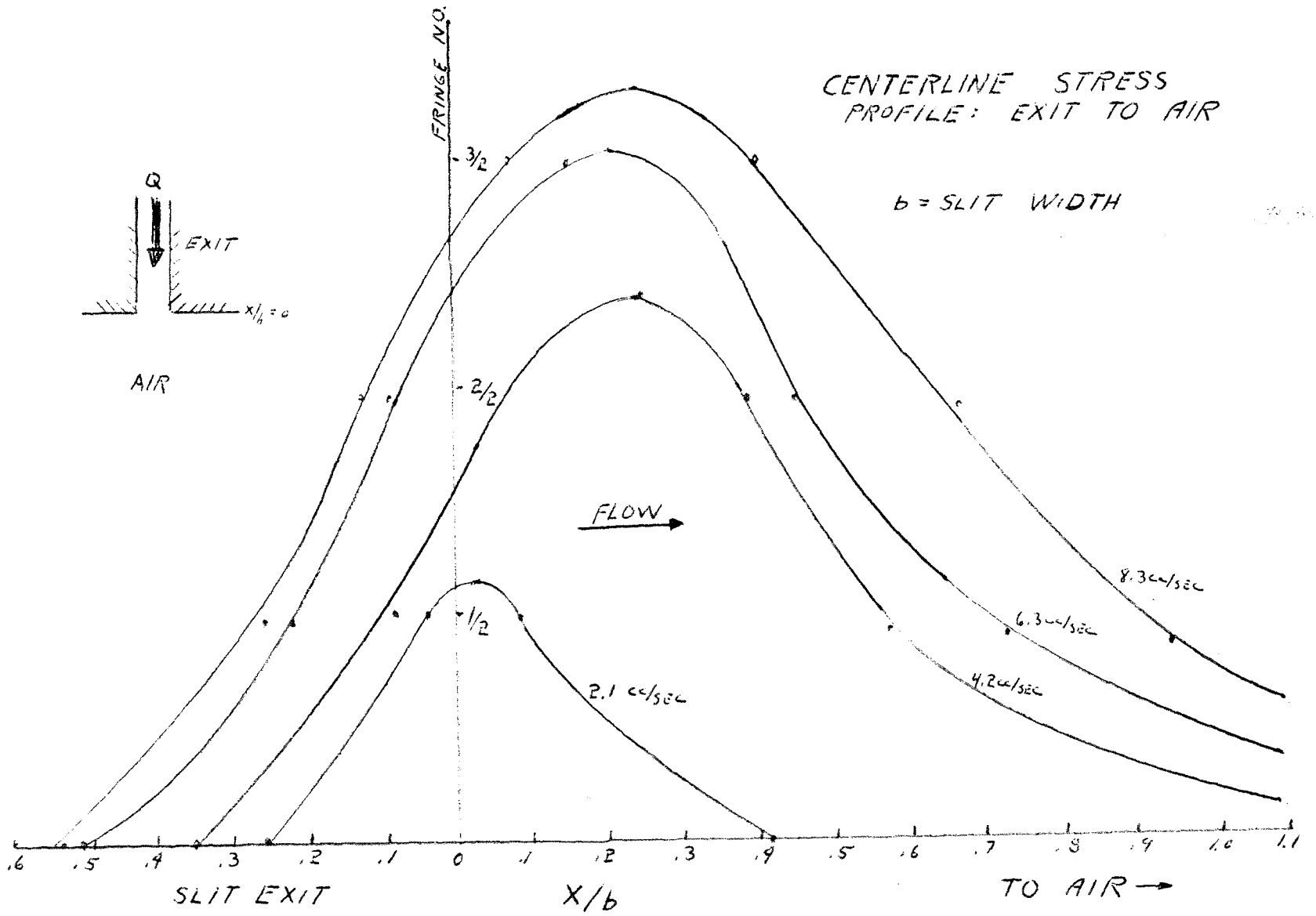
CENTERLINE STRESS
PROFILE: EXIT TO AIR
b = SLIT WIDTH
FRINGE NO.
3/2
2/2
1/2
Q
EXIT
x/b = 0
AIR
FLOW
8.3 cc/sec
6.3 cc/sec
4.2 cc/sec
2.1 cc/sec
.6 .5 .4 .3 .2 .1 0 .1 .2 .3 .4 .5 .6 .7 .8 .9 1.0 1.1
SLIT EXIT
X/b
TO AIR →

FIGURE 13

SLIT FRINGE DISTANCES FROM CENTERLINE

(values are with respect to each other)

Fringe Number	$\lambda = 4.4\times10^{-5}$	$\lambda = 3.34\times10^{-5}$	$\lambda = 2.23\times10^{-5}$	$\lambda = 1.12\times10^{-5}$
0	0	0	0	0
1	.006	.0074	.0078	.0169
2	.0122	.0146	.0175	.0327
3	.0175	.0213	.0271	
4	.0242	.0281		
5	.0298			

The slit wall is located at .0357

GRAPH 4

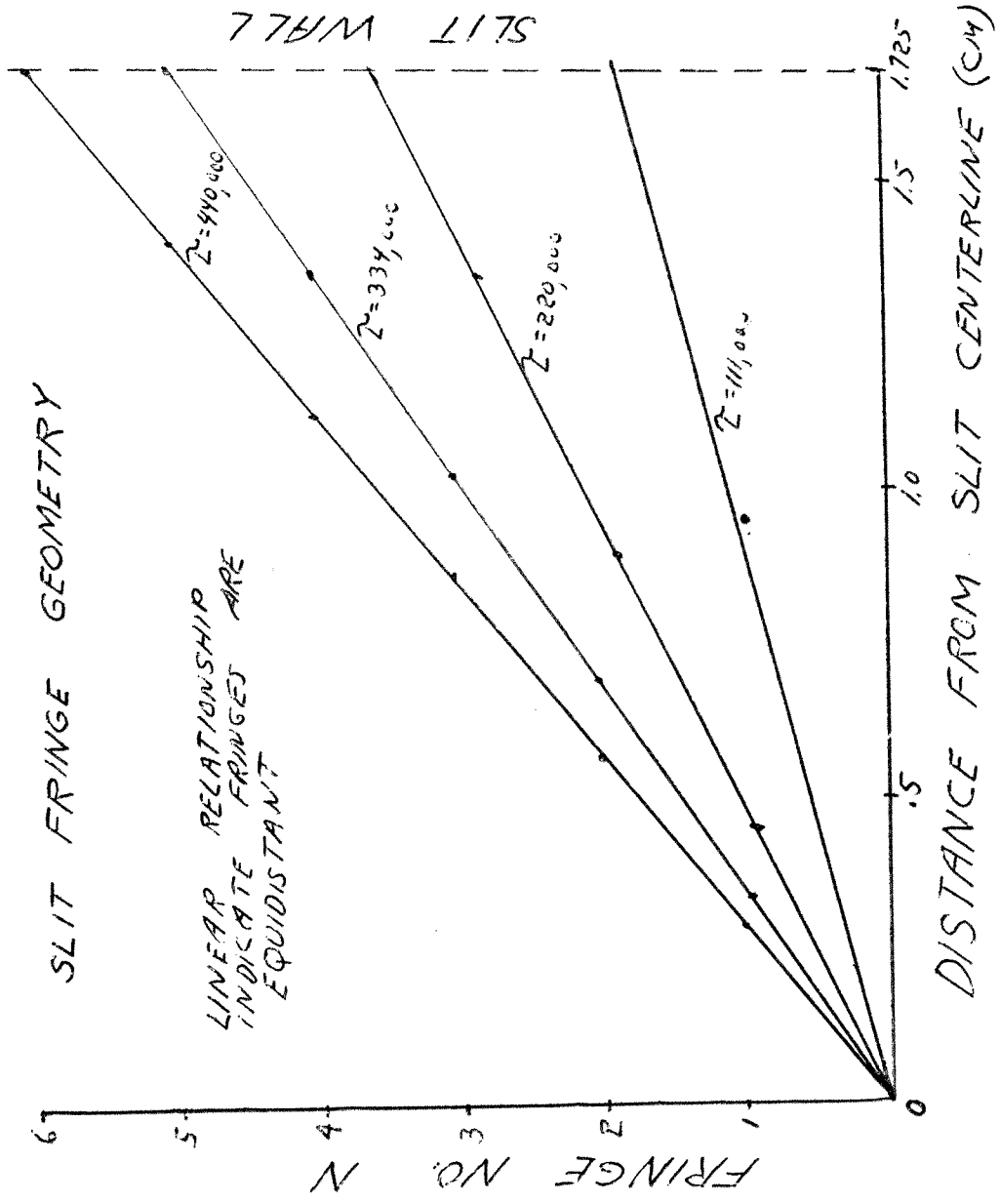
SLIT WALL
SLIT FRINGE GEOMETRY
LINEAR RELATIONSHIP INDICATE FRINGES ARE EQUIDISTANT
Z=440,000
Z=334,000
Z=220,000
Z=111,000
FRINGE NO. N
DISTANCE FROM SLIT CENTERLINE (CM)
0
.5
1.0
1.5
1.725
1
2
3
4
5
6

GRAPH 5

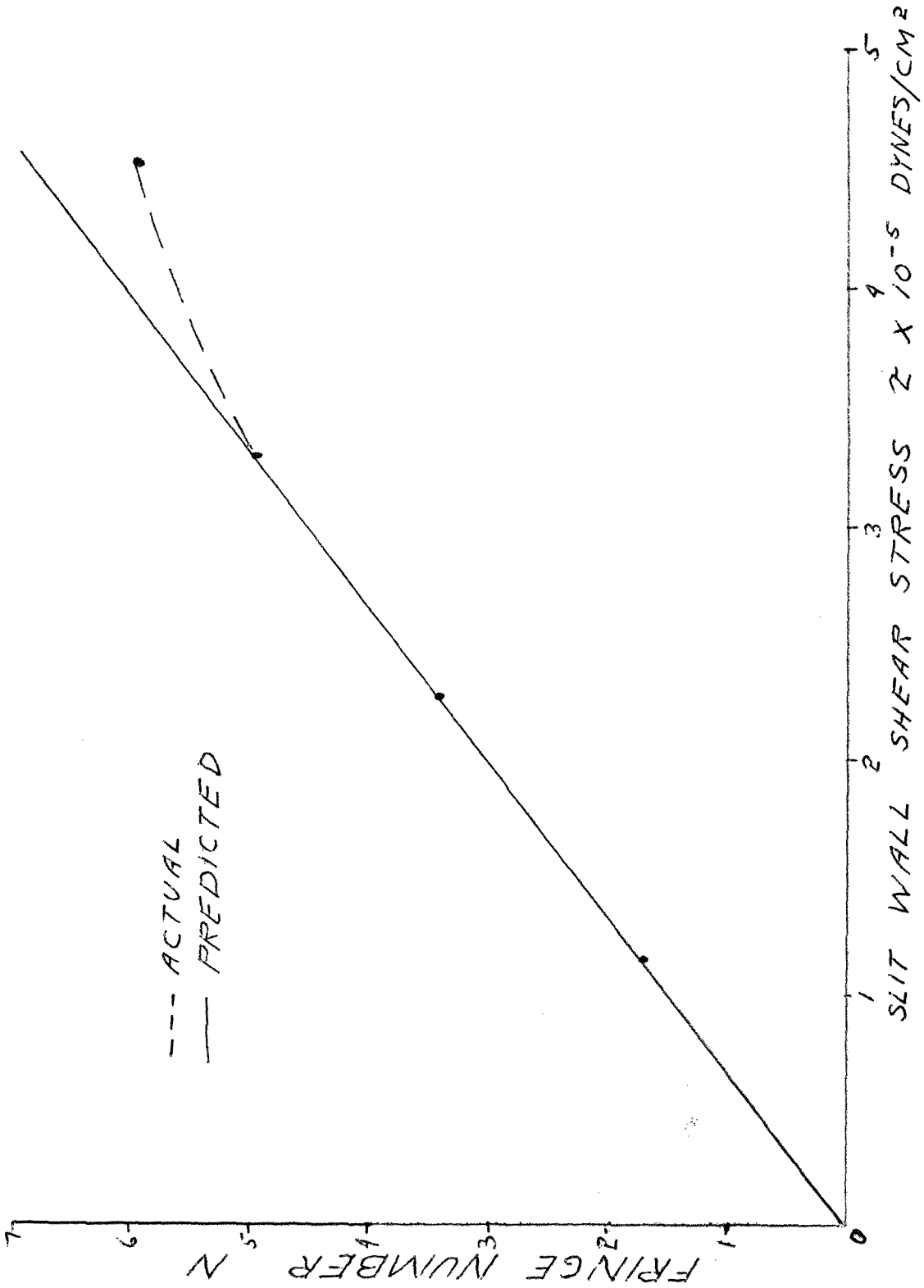
FRINGE NUMBER N
SLIT WALL SHEAR STRESS τ x 10⁻⁵ DYNES/CM²
--- ACTUAL
—— PREDICTED
0
1
2
3
4
5
6
7
1
2
3
4
5

Sequence of Fringes

N	x/b	$\sqrt{N_o/N}$	R
1/6	2.198	1	.735231
1/2	1.305	.57735	.4365225
5/6	1.0421	.4472	.3489
1	.943	.40824	.31543
$1\frac{1}{2}$	.618	.33333	.20672
2	.467	.28867	.15621
$2\frac{1}{2}$	.223	.25819	.07459

$N_o = 1/6$

$b = .3345$

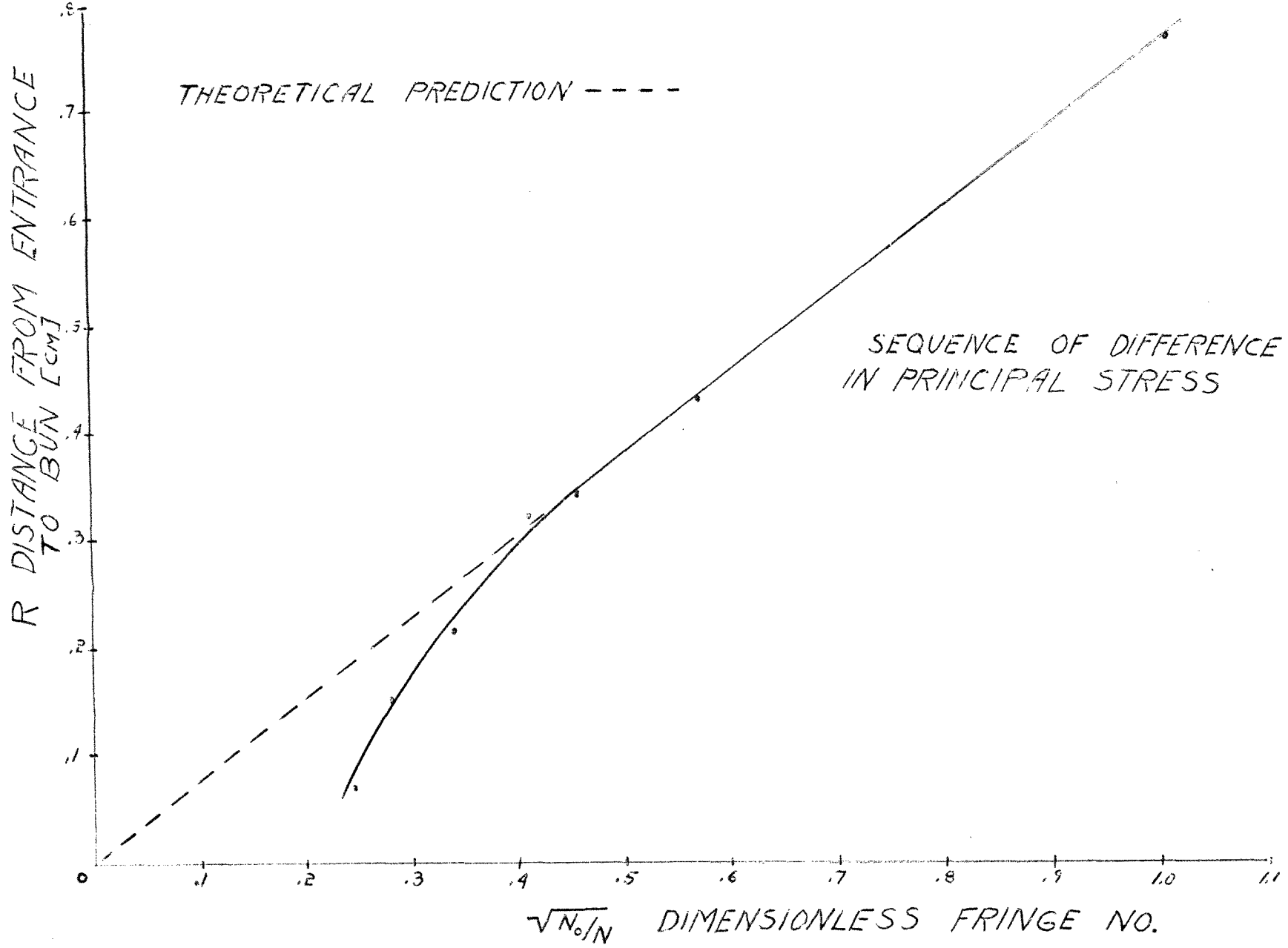
R DISTANCE FROM ENTRANCE TO BUN [CM]
THEORETICAL PREDICTION - - - -
SEQUENCE OF DIFFERENCE IN PRINCIPAL STRESS
0
.1
.2
.3
.4
.5
.6
.7
.8
.9
1.0
1.1
$\sqrt{N_o/N}$ DIMENSIONLESS FRINGE NO.

GRAPH 6

CENTERLINE POSITION OF ZERO STRESS

Slit Pressure Drop (PSI)	Distance From Slit Entrance (cm)	Centerline Velocity (cm/sec)	Time to Equilibrate (sec)
16.5	.0166	1.1	.0148
23	.0275	1.9	.0148
39.5	.0428	2.9	.0161
55.1	.0535	3.8	.0135
78.1	.0907	5.8	.0154
110	.1190	7.9	.0141
162	.1324	11.9	.0123
229	.1448	15.8	.0099

GRAPH 7

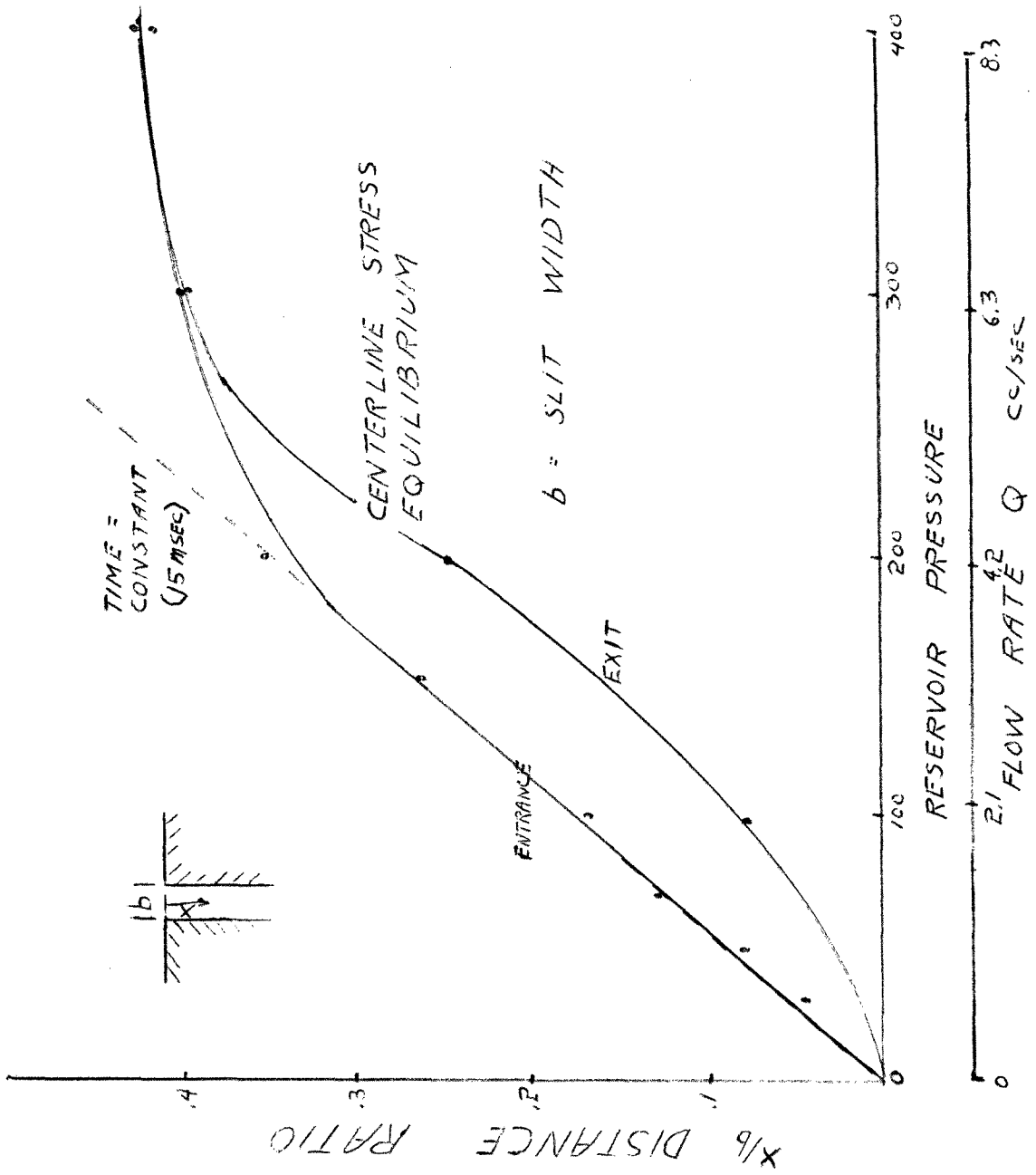
x/b DISTANCE RATIO
.4
.3
.2
.1
0
100
200
300
400
RESERVOIR PRESSURE
2.1
4.2
6.3
8.3
FLOW RATE Q cc/sec
b = SLIT WIDTH
CENTERLINE STRESS EQUILIBRIUM
EXIT
ENTRANCE
TIME = CONSTANT (15 MSEC)
b

TEMPERATURE TESTS

Utilizing the linear thermistor

Flow Time (seconds)	MV Reading (millivolts)	Temperature (degrees Fahrenheit)
0	-16.2	77.7
15	-16.5	
30	-14.8	
45	-14.2	
60	-13.8	78.3
75	-13.2	
90	-12.8	
105	-12.6	
120	-12.4	78.6
135	-12.1	
150	-11.8	
165	-11.6	
180	-11.3	78.7
195	-11.1	
210	-10.9	
225	-10.7	
240	-10.6	78.8
255	-10.2	
270	-10.1	
285	-9.99	

Flow Time (seconds)	MV Reading (millivolts)	Temperature (degrees Fahrenheit)
300	-9.97	78.9
315	-9.94	
330	-9.93	
345	-9.91	79.1

Insertion of a thermocouple into the exit so as to just contact the exiting fluid gave a 1.8 degree Fahrenheit temperature rise over a period of two minutes.

ENTRANCE VELOCITY AT CONSTANT RADIUS

Data taken from streak photographs at 4.2cc/sec.

Radius = x/b = 1

Angle to vertical (θ)	Velocity (cm/sec.)	K (cm^2/sec.)
0	———	———
3	3.118	.5818
7	———	———
13	3.06	.594
18	2.90	.594
23	———	———
28	2.52	.6015
33	2.38	.6297
38	1.931	.5787
43	1.566	.537
48	1.414	.5877
53	1.342	.6895
58	1.287	.8529
63	———	———
90	———	———
	Avg.	.5874 ± 4%

$$K = \frac{VR}{\cos^2\theta}$$

GRAPH 8

RELATIVE UPSTEAM VELOCITY PROFILE

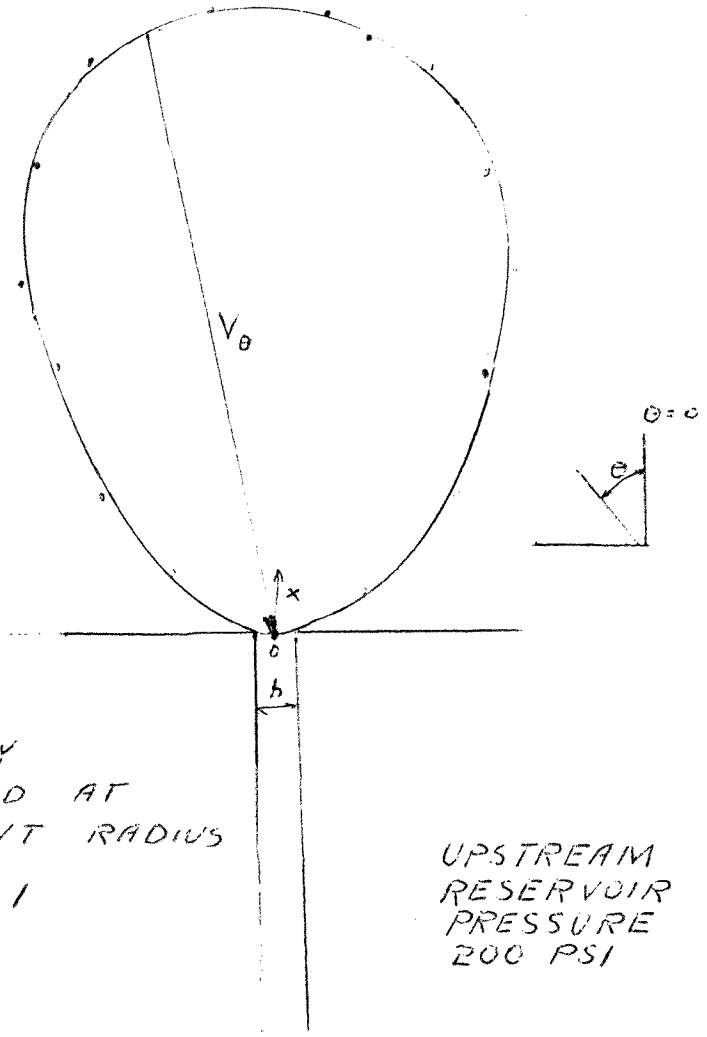

VELOCITY MEASURED AT CONSTANT RADIUS

$x/b = 1$

UPSTREAM RESERVOIR PRESSURE 200 PSI

LENGTH OF LINE FROM O TO CURVE IS INDICATIVE OF THE VELOCITY MAGNITUDE AT ANGLE θ

NOTE: FLOW IS RADIAL WITH CENTER AT O WHICH LIES WITHIN THE SLIT FOR $x/b < 3$

THEORETICAL
$V_N = \cos^{3/2}\theta$
VELOCITY ALONG
AN ISOCHROMATIC
VELOCITY (cm/sec) $\sigma_1 - \sigma_2 = \text{CONSTANT}$
$\cos^{3/2}\theta$
0
.1
.2
.3
.4
.5
.6
.7
.8
.9
1.0
.25
.5
.75
1.0
1.25
1.5

GRAPH 9

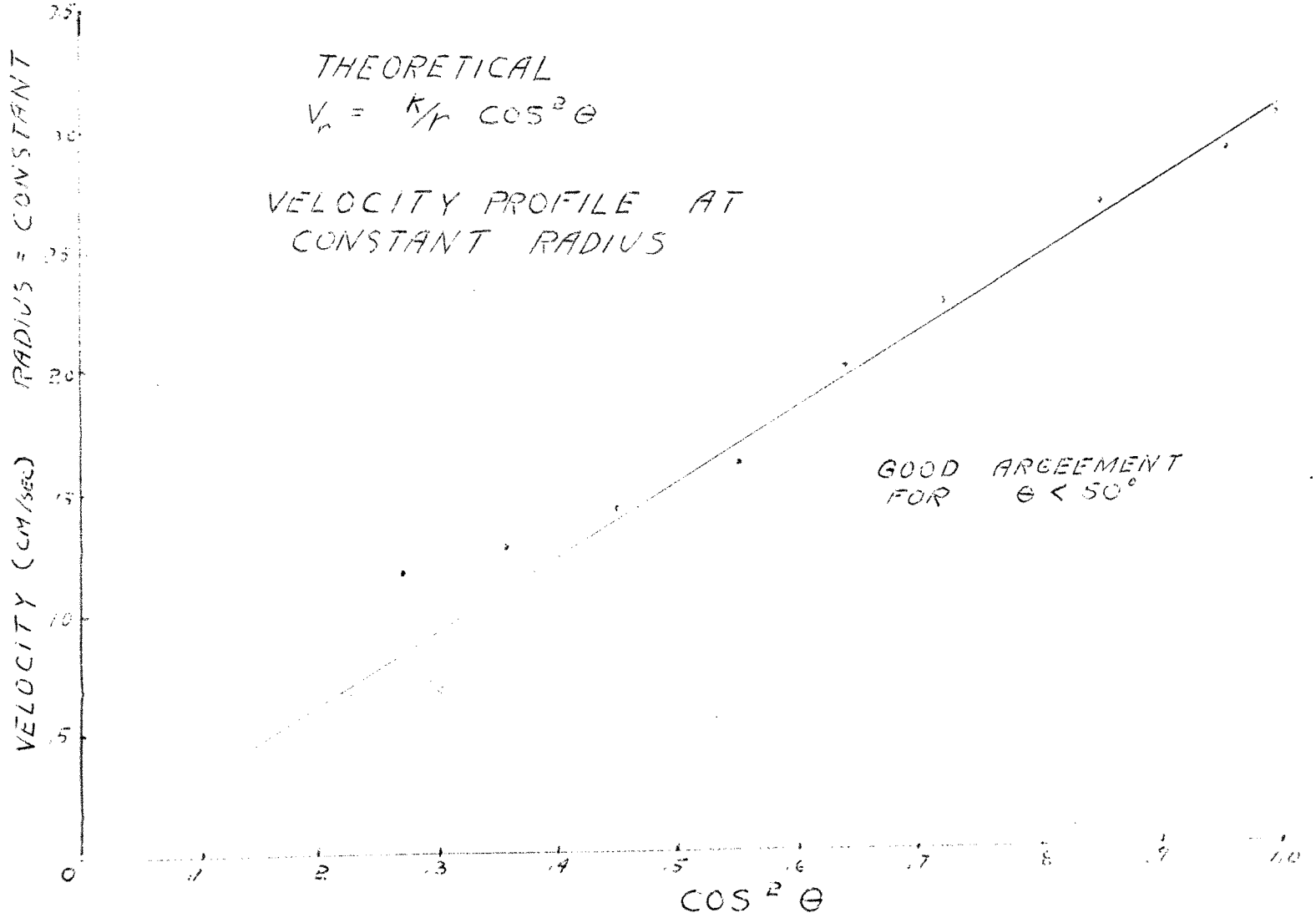
THEORETICAL
$V_r = K/r \cos^2\theta$
VELOCITY PROFILE AT CONSTANT RADIUS
GOOD AGREEMENT FOR $\theta < 50°$
VELOCITY (CM/SEC) RADIUS = CONSTANT
0
.5
1.0
2.0
2.5
.1
.2
.3
.4
.5
.6
.7
.8
.9
1.0
$\cos^2\theta$

REFERENCES

Adams, E. B., J. C. Whitehead, and D. C. Bogue. "Stresses in a Viscoelastic Fluid in Converging and Diverging Flow," AiChe Journal, XI (1965), 1026.

Arai, Teikichi, Hideki Asano, Hirotaka Ishikawa, Jun Mizutani, and Shinji Murai, "Flow Patterns and Principal Stress Lines for Molten Polyethylene in the Entrance Region of a Parallel Slit," Chemistry of High Polymers, The Society of Polymer Science, Japan, XXIX, No. 330, (Oct. 1972), 743-747.

Arai, Teikichi, and Hideki Asano. "Analysis of the Flow of Molten Polyethylene Through a Parallel Slit by the Flow Birefringence Method," The Society of Polymer Science, Japan, XXIX, No. 327, (July 1972), 510-514.

Bogue, D. C., and F. N. Peebles. "Birefringent Techniques in Two Dimensional Flow," Transactions of the Society of Rheology, VI (1962), 317.

Buteau, Leon. "Lecture Notes on Photoelasticity," Newark College of Engineering, Newark, N. J., (1973).

Drexler, Leonard H., and Chang Dae Han. "Studies of Converging Flows of Viscoelastic Polymeric Melts Part II. Velocity Measurements in the Entrance Region of a Sharp-Edged Slit Die," Transactions of the Society of Rheology, XVII (1973).

Fields, T. R., and D. C. Bogue. "Stress Birefringent Patterns of a Viscoelastic Fluid at a Sharp-Edged Entrance," Transactions of the Society of Rheology, XII (1968), 39.

Fourney, M. E. "Application of Holography to Photoelasticity," Experimental Mechanics, (Jan. 1968), pp. 33-38.

Frantisak, F., Palade De Iribarne, J. W. Smith, R. L. Hummel. "Nondisturbing Tracer Technique for Quantitative Measurements in Turbulent Flow," Industrial Engineering Chemical Fundamental, VIII (1969), 160.

Frocht, M. Photoelasticity, vol. 1, John Wiley and Sons, Inc., New York, N. Y. (1941).

Funatsu, Kazumori, and Yoshiro Mori. "Viscoelastic Stresses in the Flow of Polymer Melt," Chemistry of High Polymers, The Society of Polymer Science, Japan, XXV, No. 278, (1968).

Funatsu, K., and Y. Mori. "On Viscoelastic Flow of a Molten Polymer," Chemistry of High Polymers, The Society of Polymer Science, Japan, XXV, No. 279, (1968), 337.

Gerrard, J. E., F. E. Steidler, and J. K. Appeldorn. "Viscous Heating in Capillaries," I&EC Fundamentals, IV (August 1965), 332.

Han, C. D., M. Charles, and W. Philippoff. "Measurement of the Axial Pressure Distribution of Molten Polymers in Flow Through a Circular Tube," Transactions of the Society of Rheology, XIII (1969), 455.

Han, Chang Dae, and Leonard H. Drexler. "Studies of Converging Flows of Viscoelastic Polymeric Melts, Part I. Stress-Birefringent Measurements in the Entrance Region of a Sharp-Edged Slit Die," Transactions of the Society of Rheology, XVII (1973).

Janeschitz-Kriegl, H. "On the Technique of Measuring Flow Birefringence," Journal of Polymer Science, XXIII (1957), 181-188.

Jessop, H. T. "On the Tardy and Sēnarmont Methods of Measuring Fractional Relative Retardations," British Journal of Applied Physics, (May 1953), pp. 138-141.

Lodge, A. S. "Variation of Flow Birefringence with Stress," Nature, CLXXVI (1955), 838.

Murai, Hokuro, Yoshiro Mori, and Youichi Mikami. "Flow Birefringence of Molten Polyethylene," Journal of the Society of Materials Science, XVI, No. 166, (July 1967), 562-566.

Oka, Syoten. "The Steady Slow Motion of a Viscous Fluid Through a Tapered Tube," Journal of the Physical Society of Japan, XIX (August 1964), 1481-1484.

Philippoff, W. "Flow Birefringence and Stress," Journal of Applied Physics, XXVII (1956), 984.

Philippoff, W. "On Normal Stresses, Flow Curves, Flow Birefringence, and Normal Stresses of Polyisobutylene Solutions, Part I Fundamental Principles," Transactions of the Society of Rheology, I (1957), 95.

Philippoff, W. Personal Conversation, Newark College of Engineering, Newark, N. J., (January - December, 1973).

Philippoff, W. "The Present Stand of Rheo-Optics of Polymer Solutions," Reprinted from Proceedings of the Fifth International Congress of Rheology, IV (1970).

Philippoff, W. "The Temperature Dependence of Flow Birefringence Parameters," Transactions of the Society of Rheology, III (1959), 153-160.

Philippoff, W. Nature, 178 (1956), 811.

Post, D. "Isochromatic Fringe Sharpening and Fringe Multiplication in Photoelasticity," Proceedings of the Society for Experimental Stress Analysis, XII, No. 2 (1955), 143-156.

Prados, J. W., and F. N. Peebles. "Two Dimensional Laminar-Flow Analysis Utilizing a Doubly Refracting Liquid," AiChe Journal, V (1959), 225.

Rea, David R., and W. R. Schowalter. "Velocity Profiles of a Non-Newtonian Fluid in Helical Flow," Transactions of the Society of Rheology, XI-1 (1967), 125-143.

Sanford, R. J., and A. J. Durelli. "Interpretation of Fringes in Stress-Holo-Interferometry," Experimental Mechanics, (April 1971), pp. 161-166.

Wales, J. L. S. "Apparatus for the Measurement of Flow Birefringence of Polymer Melts at High Shear Stresses," Rheological Acta, VIII (1969), 38.